6. Bunge, R. P., Bunge, M. B. & Eldridge, C. F. *A. Rev. Neurosci.* **9,** 305–328 (1986).
7. Muir, D., Gennrich, C., Varon, S. & Manthorpe, M. *Neurochem. Res.* **14,** 1003–1012 (1989).
8. Acheson, A., Barker, P. A., Alderson, R. F., Miller, F. D. & Murphy, R. A. *Neuron* **7,** 265–275 (1991).
9. Baehr, M. & Bunge, R. P. *Expl Neurol.* **106,** 27–40 (1989).
10. Matsuoka, I., Meyer, M. & Thoenen, H. *J. Neurosci.* **11,** 3165–3177 (1991).
11. Bhattacharyya, A. *et al. J. Neurobiol.* **23,** 451–466 (1992).
12. Aguayo, A. J. *et al. Brain Res.* **104,** 1–20 (1976).
13. Salzer, J. L., Williams, A. K., Glaser, L. & Bunge, R. P. *J. Cell Biol.* **84,** 753–766 (1980).
14. Baichwal, R. R., Bigbee, J. W. & DeVries, G. W. *Proc. natn. Acad. Sci. U.S.A.* **85,** 1701–1705 (1988).
15. Lu, X. & Richardson, P. M. *J. Neurosci.* **11,** 972–978 (1992).
16. Pellegrino, R. G., Politis, M. J., Ritchie, J. M. & Spencer, P. S. *J. Neurocytol.* **15,** 17–28 (1986).
17. Salzer, J. L. & Bunge, R. P. *J. Cell Biol.* **84,** 739–752 (1980).
18. Brockes, J. P. *Science* **225,** 1280–1287 (1984).
19. Sandrock, A. W. Jr & Matthew, W. D. *Brain Res.* **425,** 360–363 (1987).
20. Sendtner, M., Stöckli, K. A. & Thoenen, H. *J. Cell Biol.* **118,** 139–148 (1992).
21. Raff, M. C., Abney, E., Brockes, J. P. & Hornby-Smith, A. *Cell* **15,** 813–822 (1978).
22. Lemke, G. E. & Brockes, J. P. *J. Neurosci.* **4,** 75–83 (1984).
23. Holmes, W. E. *et al. Science* **256,** 1205–1210 (1992).
24. Wen, D. *et al. Cell* **69,** 559–572 (1992).
25. Doolittle, R. F., Feng, D. F. & Johnson, M. S. *Nature* **307,** 558–560 (1984).
26. Williams, A. F. & Barclay, A. N. *A. Rev. Immun.* **6,** 381–405 (1988).
27. Kallunki, P. & Tryggvason, K. *J. Cell Biol.* **116,** 559–571 (1992).
28. Chan, A. M.-L. *et al. Science* **254,** 1382–1385 (1991).
29. Yarden, Y. & Ullrich, A. *A. Rev. Biochem.* **57,** 443–478 (1988).
30. Ullrich, A. & Schlessinger, J. *Cell* **61,** 203–212 (1990).
31. Schlessinger, J. & Ullrich, A. *Neuron* **9,** 383–391 (1992).
32. Schechter, A. L. *et al. Nature* **312,** 513–516 (1984).
33. Ullrich, A. *et al. Nature* **309,** 418–425 (1984).
34. Kraus, M. H., Issing, W., Miki, T. & Popescu, N. C. *Proc. natn. Acad. Sci. U.S.A.* **86,** 9193–9197 (1986).
35. Cohen, J. A., Yachnis, A. T., Arai, M., Davis, J. G. & Scherer, S. S. *J. Neurosci. Res.* **31,** 622–634 (1992).
36. Davis, J. B. & Stroobant, P. *J. Cell Biol.* **110,** 1353–1360 (1990).
37. Altman, J. & Bayer, S. A. in *Advances in Anatomy Embryology and Cell Biology* Vol. 85 *The Development of the Rat Spinal Cord* (Springer, Berlin, 1984).
38. Falls, D. L., Rosen, K. M., Corfas, G., Lane, W. S. & Fischbach, G. D. *Cell* **72,** 801–815 (1993).
39. Schwab, M. E. & Thoenen, H. *J. Neurosci.* **5,** 2415–2423 (1985).
40. Aguayo, A. J. in *Synaptic Plasticity* 457–484 (Guilford, New York, 1985).
41. Nordlund, M., Hong, D.-M., Fei, X. & Ratner, N. *Glia* **5,** 182–192 (1992).
42. Brockes, J. P., Breakefield, X. O. & Martuza, R. L. *Ann. Neurol.* **20,** 317–321 (1986).
43. Perantoni, A. O., Rice, J. M., Reed, C. D., Watatani, M. & Wenk, M. L. *Proc. natn. Acad. Sci. U.S.A.* **84,** 6317–6321 (1987).
44. Nikitin, A. Y., Ballering, L. A. P., Lyons, J. & Rajewsky, M. F. *Proc. natn. Acad. Sci. U.S.A.* **88,** 9939–9943 (1991).
45. Lupu, R., Dickson, R. B. & Lippman, M. E. *J. Ster. Biochem. molec. Biol.* **43,** 229–236 (1992).
46. Chirgwin, J. M., Przybyla, A. E., MacDonald, R. J. & Rutter, W. J. *Biochemistry* **18,** 5294–5299 (1979).
47. Frohman, M., Dush, M. & Martin, G. *Proc. natn. Acad. Sci. U.S.A.* **85,** 8998 (1988).
48. Sambrook, J., Fritsch, E. F. & Maniatis, T. in *Molecular Cloning. A Laboratory Manual 2nd edn* (Cold Spring Harbor Laboratory press, Cold Spring harbor, New York, 1989).
49. Wilkinson, D. G., Bailes, J. A. & McMahon, A. P. *Cell* **50,** 79–88 (1987).
50. Takebe, Y. *et al. Molec. cell. Biol.* **8,** 466–472 (1988).
51. Brockes, J. P., Fields, K. L. & Raff, M. C. *Brain Res.* **165,** 105–118 (1979).

ACKNOWLEDGEMENTS. We thank M. Alfano, G. Gao, J. Lucas, C. Nolan, M. Rossi and O. Truong for technical assistance; G. Fischbach for sharing unpublished results. D. Anderson, J. Brockes, A. Davies, H. Goodman, T. Jessell, R. Kamen, S. J. Lee, M. Noble and A. Server for discussion; L. Guarente for comments on the manuscript; and M. A. Carr for preparing it.

SNAP receptors implicated in vesicle targeting and fusion

Thomas Söllner, Sidney W. Whiteheart, Michael Brunner, Hediye Erdjument-Bromage, Scott Geromanos, Paul Tempst & James E. Rothman

Rockefeller Research Laboratory, Memorial Sloan-Kettering Cancer Center, 1275 York Avenue, New York, New York 10021, USA

The *N*-ethylmaleimide-sensitive fusion protein (NSF) and the soluble NSF attachment proteins (SNAPs) appear to be essential components of the intracellular membrane fusion apparatus. An affinity purification procedure based on the natural binding of these proteins to their targets was used to isolate SNAP receptors (SNAREs) from bovine brain. Remarkably, the four principal proteins isolated were all proteins associated with the synapse, with one type located in the synaptic vesicle and another in the plasma membrane, suggesting a simple mechanism for vesicle docking. The existence of numerous SNARE-related proteins, each apparently specific for a single kind of vesicle or target membrane, indicates that NSF and SNAPs may be universal components of a vesicle fusion apparatus common to both constitutive and regulated fusion (including neurotransmitter release), in which the SNAREs may help to ensure vesicle-to-target specificity.

TRANSACTIONS among the membrane-bound compartments in the cytoplasm of eukaryotic cells are generally executed by transport vesicles which bud from one membrane and fuse selectively with another[1]. The mechanism by which each vesicle chooses its target is currently unknown, but must embody the essence of compartmental specificity. Choice of target is implicit in all vesicular fusion events, from the ubiquitous steps in the constitutive secretory and endocytotic pathways (such as the fusion of a vesicle from the endoplasmic reticulum with the Golgi) to specialized and tightly regulated forms of exocytosis (such as the triggered fusion of a synaptic vesicle containing neurotransmitter with the axonal membrane). Here we describe a fundamental relationship between these processes, suggesting that a general apparatus is used to bring about fusion, and that specificity is established by the pairing of compartment-specific proteins in the transport vesicle and target membrane, respectively.

The *N*-ethylmaleimide-sensitive fusion protein is a soluble tetramer of 76K subunits which was purified[2,3] on the basis of its ability to restore intercisternal Golgi transport in a cell-free system[4,5]. It is required for transport vesicle fusion, as vesicles accumulate at the acceptor membrane in its absence[6,7]. In yeast, NSF is encoded by the *SEC18* gene[8], originally shown to be necessary for transport from the endoplasmic reticulum (ER) to the Golgi[9]. The *SEC18* protein can replace NSF in a mammalian system for cell-free Golgi transport[8] and is required at every discernible step of the secretory pathway *in vivo*[10]. NSF thus appears to participate in a variety of intracellular fusion processes.

NSF requires additional cytoplasmic factors to attach to Golgi membranes[11]. Three species of monomeric soluble NSF attachment proteins, termed α-, β- and γ-SNAP (M_rs of 35, 36 and 39K, respectively), have been purified from brain[12,13] and SNAP activity is necessary for vesicle fusion *in vitro*[13]. α-SNAP (but not β- or γ-SNAP) can restore animal cell Golgi transport activity to cytosol prepared from *sec17* mutant yeast, implying[13] that the *SEC17* gene encodes α-SNAP in yeast. SEC17 is now known to be functionally equivalent to α-SNAP[14], and the two proteins are clearly related[15]. In the absence of functional SEC17 (or SEC18), ER to Golgi transport stops in yeast, and transport

vesicles accumulate[16]. SNAPs, like NSF, thus appear to be components of a general intracellular membrane fusion apparatus common to all eukaryotic cells.

SNAPs bind to distinct sites in membranes which up until now have only been operationally defined, and NSF will only interact with SNAPs that are already attached to these sites[17]. α-SNAP and β-SNAP compete for binding to the same receptor site with low nM affinity. γ-SNAP binds to a noncompetitive site in the same complex[17], and, although not essential for NSF binding, increases the complexes' affinity for NSF[18]. Crosslinking studies suggest that the SNAP receptor contains an α-SNAP-binding subunit of 30-40K (ref. 17). When membrane-bound NSF-SNAP-SNAP receptor complexes are solubilized with detergent, they sediment as a distinct multisubunit particle at 20S (ref. 18), which may form the core of a generalized apparatus catalysing bilayer fusion at its point of assembly[6,13]. The 20S particles are also formed when detergent extracts of Golgi membranes containing SNAP receptors are mixed with SNAPs and NSF. When NSF and SNAPs are added in excess, all SNAP receptor activity in the membrane extract is incorporated into 20S particles[18].

NSF is an ATPase containing two ATP-binding sites in separate domains[19], and the binding and hydrolysis of ATP are critical in determining the stability of NSF[3] and its attachment to membranes[2,18]. Stable 20S particles can be formed in the presence of either Mg-ATP-γS (a non-hydrolysable analogue of ATP) or ATP without magnesium. In the presence of Mg-ATP, however, particles rapidly dissociate even at 0 °C, liberating NSF in a process that requires ATP hydrolysis[18]. This disassembly may be an intrinsic step in the fusion mechanism[18].

Purification of SNAP receptors

To purify SNAP receptors, we used the specificity inherent in the assembly and disassembly of 20S particles as the basis of an affinity purification technique (schematized in Fig. 1): 20S particles were formed and attached to a solid matrix, allowing purified SNAP receptor to be released by particle disassembly when ATP was subsequently hydrolysed.

A recombinant form of NSF, epitope-tagged with a Myc peptide[20] (EQKLISEEDL) at its carboxy terminus, was expressed in *E. coli* and shown to be functional[21]. The 20S particles were formed in solution by mixing a Triton X-100 extract of membranes with pure, recombinant α- and γ-SNAPS expressed in *E. coli* and NSF-Myc at 0 °C (ref. 15) in the presence of ATP-γS and EDTA (to chelate any magnesium). A monoclonal anti-Myc IgG (9E10; ref. 22) attached to protein G beads was then added to bind the 20S particles through their NSF-Myc subunits. The anti-Myc IgG does not inhibit NSF-Myc function in cell-free transport assays (our unpublished results).

The beads were formed into a column and washed extensively before a first (nonspecific) elution with Mg-ATP-γS to elute any proteins attached in a Mg^{2+}-sensitive fashion, or by Mg-ATP-γS *per se*. A second (specific) elution was then done with Mg-ATP (replacing Mg-ATP-γS). Only proteins released as the immediate consequence of ATP hydrolysis on the column will be recovered in this specific eluate. This scheme is based on that described previously[18] but includes a number of key modifications detailed in the figure legends. As NSF remains on the beads, the specific eluate should consist of a fraction of the added SNAPs, together with additional polypeptides representing SNAP receptors, ideally in stoichiometric amounts.

A detergent extract of a crude, salt-washed total particulate fraction from the grey matter of bovine brain was used as the source of potential SNAP receptors. Membranes were washed with 1 M KCl before use to remove most of their endogenous SNAP supply[12]. As recombinant SNAPs were added in great excess for the binding reaction (Fig. 1), these should compete out the remaining endogenous SNAPs, preventing them from forming particles on the beads. Figure 2*a* shows a Coomassie blue-stained SDS-urea-high Tris-polyacrylamide gel of the specific eluate (lane 3), the nonspecific eluate fraction (lane 2), and the specific eluate from a control experiment omitting NSF-Myc (lane 1). Several bands (labelled A-F) appear only in the specific (Mg-ATP) eluate and depend on the presence of NSF. A set of bands at about M_r 70K are present in all three lanes, but apart from these, bands A-F are substantially pure in the specific eluate fraction. Band F runs as a sharper band in a standard Laemmli gel (Fig. 2*b*; specific eluate, stained with silver) than in the high Tris-urea gel (Fig. 2*a*). Bands A and C virtually co-electrophorese with the abundant band D in a Laemmli gel (Fig. 2*b*; see below).

Identification of SNAP receptors

To identify specific bands, they were excised from blots and digested with trypsin, giving peptides that were then separated by high-pressure liquid chromatography and microsequenced (see Fig. 3 for details). Bands B and D co-electrophoresed with recombinant γ-SNAP and α-SNAP, respectively, both of which were His_6-tagged[15] and thus slightly larger than their endogenous counterparts (not shown). These identifications were confirmed by microsequencing peptides from bands B and D (not shown).

Sequences from six major peptides containing a total of 70 residues were obtained from band A, each precisely matching the sequence of syntaxin B (p35B) from rat brain[23] (Fig. 3*b*). The sequences of these and peptides from the other specific bands are shown in association with the band from which they were obtained (Fig. 3*a*). No sequences or fragments attributable to any other protein were found, indicating that the bulk of material in band A is syntaxin B.

Five major peptides containing a total of 53 residues were sequenced from band C (Fig. 3*a*), and proved to differ at only one position from the published sequence of syntaxin A from rat brain[23]; the difference presumably reflects the species involved. Expected sequence differences between the 84% identical syntaxins A and B were found in the peptides from bands C and A (Fig. 3*b*). The syntaxins run more slowly than expected from their relative molecular masses (about 35K) in the high percentage Tris-SDS-urea-polyacrylamide gels were used,

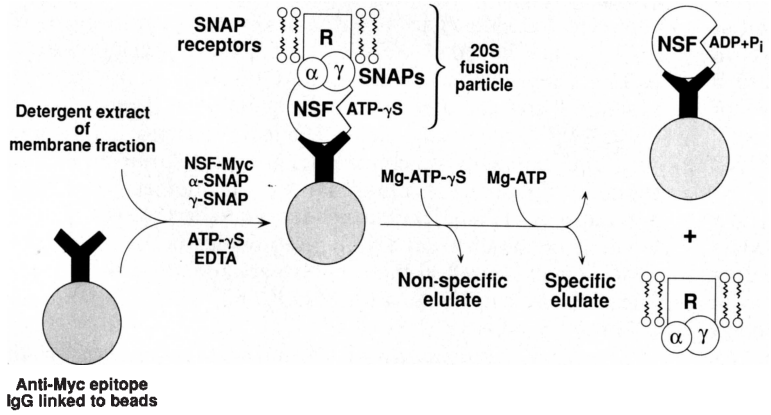

FIG. 1 Procedure used to purify SNAP receptors (SNAREs). Recombinant NSF, α-SNAP, and γ-SNAP are assembled into 20S particles by SNAREs present in a crude detergent extract of membranes. The SNAREs are incorporated stoichiometrically into the particles, which are then bound to beads by means of NSF. For this purpose, the NSF is epitope-tagged with Myc, and an anti-Myc monoclonal IgG is linked to the beads. The beads are washed and then eluted first with Mg-ATP-γS (nonspecific eluate) and then with Mg-ATP (specific eluate). The bound 20S particles disassemble in the presence of Mg-ATP (but not Mg-ATP-γS), releasing stoichiometric amounts of SNAPs and SHAREs. NSF remains bound to the beads. Experimental details are given in Fig. 2 legend.

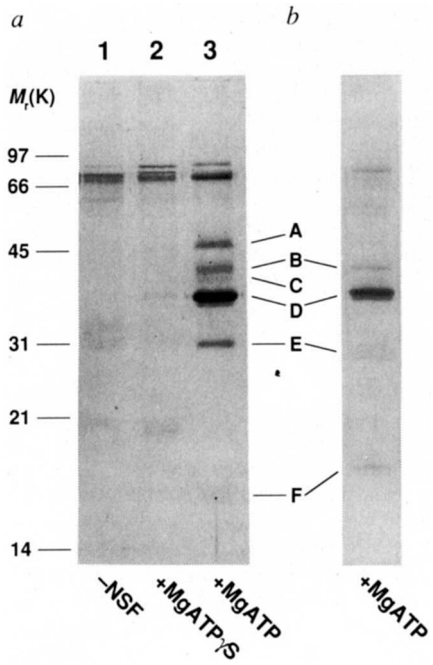

FIG. 2 Identification of proteins released from NSF after ATP hydrolysis. *a*, Polyacrylamide gel stained with Coomassie blue. Lane 1, control, Mg–ATP eluate of control binding reaction in the absence of NSF; lane 2, 'nonspecific' eluate from complete binding reaction with NSF–Myc and Mg–ATP-γS; lane 3, 'specific' eluate of the same column as for lane 2 following the exchange of ATP for ATP-γS (in the presence of EDTA) and addition of Mg^{2+} to allow ATP hydrolysis (Fig. 1). *b*, Silver-stained Laemmli gel of the specific (Mg–ATP) eluate.

METHODS. All manipulations were performed at 0–4 °C. Bovine brain tissue was initially stripped of meninges, and all but the grey matter removed and discarded. The resulting tissue (30g) was homogenized with 30 strokes of a Dounce homogenizer in buffer A (20 mM Tris–HCl, pH 8.0, 1 M KCl, 250 mM sucrose, 2 mM $MgCl_2$, 1 mM DTT, 1 mM phenylmethylsulphonyl fluoride (PMSF). A total particulate fraction was isolated by centrifugation in a Ti45 rotor (Beckman) for 60 min at 33,000 r.p.m. The pellet was then resuspended in buffer A by Dounce homogenization and the membranes collected by centrifugation. The resulting pellet was washed once in buffer B (10 mM HEPES/KOH, pH 7.8, 100 mM KCl, 2 mM $MgCl_2$, 1 mM DTT) and then resuspended in 100 ml buffer B. Triton X-100 was added slowly with mixing to a final concentration of 4% (v/v), and the suspension incubated on ice with frequent mixing. After 45 min, the suspension was clarified by centrifugation (Ti-45 rotor) for 60 min at 33,000 r.p.m. and the supernatant dialysed overnight against 100 vol 25 mM Tris–HCl, pH 7.8, 50 mM KCl, 1 mM DTT, 1% (v/v) Triton X-100. After dialysis, the material was clarified by centrifugation (Ti-45 rotor for 60 min at 33,000 r.p.m.), aliquoted, and stored at −80 °C. Protein concentration was measured using the BCA reaction (Pierce) with ovalbumin as standard. This bovine brain extract (2mg protein) was preincubated in the presence of His_6-α-SNAP (12 μg protein), His_6-γ-SNAP (4 μg protein) and NSF–Myc (12 μg protein) in buffer C (25 mM HEPES/KOH, pH 7.0, 0.75% (w/v) Triton X-100, 75 mM KCl, 1 mM DTT, 2 mM EDTA, 0.5 mM ATP (for lane 1) or 0.5 mM ATP-γS (for lanes 2 and 3), 1% (w/v) polyethyleneglycol (PEG) 4,000, 0.4 mM PMSF) for 30 min at 4 °C in a final volume of 2 ml. Mouse anti-Myc monoclonal antibody (200 μg protein, termed 9E10; ref. 22) covalently coupled to protein G–Sepharose 4 fast-flow (Pharmacia) was added and the incubation continued for 2 h with constant agitation. (The anti-Myc IgG was covalently coupled to the protein G–Sepharose using 20 mM dimethylsuberimidate as described[47].) The beads were packed into a column, washed with 10 vol buffer D (20mM HEPES/KOH, pH 7.0, 0.5% (w/v) Triton X-100, 100 mM KCl, 1 mM DTT, 2 mM EDTA, 0.5 mM ATP (lane 1) or 0.5 mM ATP-γS (lanes 2 and 3), 0.4mM PMSF) and the proteins eluted with 6 column-volumes of buffer D containing 8 mM $MgCl_2$ (resulting in a concentration of free Mg^{2+} of 4 mM). The column containing ATP-γS (lanes 2 and 3) was washed with an additional 2 column-volumes of buffer D containing 4 mM EDTA to complex the free Mg^{2+}, 3 column-volumes of buffer D containing ATP to exchange for bound ATP-γS, and then eluted with 6 column-volumes of buffer D containing 8 mM $MgCl_2$ to allow ATP hydrolysis. The appropriate fractions containing the eluate were pooled, precipitated with trichloroacetic acid, boiled in sample buffer[48] and analysed by electrophoresis on Tris–urea/SDS–polyacrylamide (18% acrylamide, 6M urea, 750 mM Tris–HCl, pH 8.85, 50 mM NaCl, 0.1% SDS[49]) and stained with Coomassie blue R-250. For sequencing, the reaction was scaled up 25-fold.

although they virtually co-electrophorese with α-SNAP (35K) in standard Laemmli gels (Fig. 2*b*, and data not shown).

Three major peptides (Fig. 3*a*) from band E gave sequences (Fig. 3*c*) matching a protein predicted from a mouse brain complementary DNA clone which by coincidence has been termed SNAP-25 (for synaptosome-associated protein of 25K; ref. 24). Of 45 residues obtained, 42 were identical to the published sequence of mouse SNAP-25. The discrepancies, two of which are conservative, are probably due to species differences. SNAP-25 migrates at M_r 31K in the SDS–urea gel.

All five peptides (containing 43 identified residues) sequenced from band F (Fig. 3*a*) exactly matched the sequence of VAMP/synaptobrevin-2 from bovine brain[25] (Fig. 3*d*). VAMP-2, the major isoform of VAMP/synaptobrevin in brain, differs slightly from VAMP-1 (refs 26, 27); all the sequences obtained from band F correspond to VAMP-2. All HPLC peptide peaks from band F, other than those attributable to trypsin autodigestion, were shown to be derived from VAMP/synaptobrevin. As a control, the region corresponding to band F from the blot of the gel of the nonspecific (Mg–ATP-γS) eluate was subject to tryptic digestion and HPLC analysis in parallel with band F from the Mg–ATP eluate in two separate experiments. None of the VAMP/synaptobrevin-2 peptide peaks from band F were present in the HPLC profile of the control; only the autolytic tryptic peptides were detected.

Two peptides from the digest of band F failed to give any sequence, suggesting that they had blocked N termini. Mass spectroscopy indicated that these components had m/z values of 2,680.90 and 2,838.36 respectively, differing by 157.46, or approximately the molecular mass of Arg (156.19 average isotopic mass). The tryptic cleavage site closest to the N terminus in bovine VAMP/synaptobrevin-2 consists of an Arg–Arg sequence (at positions 30–31), so the expected partial cleavage would yield two N-terminal-derived peptides. If it is assumed that the initiator Met is removed, and that the newly generated N-terminal Ser is acetylated, adding 42.04 to the M_r, the two masses correspond almost perfectly with the predicted M_rs $[MH^+]$ of the bovine VAMP/synaptobrevin-2 peptides spanning residues 2–30 and 2–31 (2,681.90 and 2,838.09, respectively). The N terminus of VAMP/synaptobrevin-2 thus appears to be processed and acetylated.

The material in the 70K region of all three eluates (specific, nonspecific and control) (Fig. 2) was microsequenced (from the specific eluate) in an attempt to determine if any synaptotagmin/p65 was present, as this protein can be immunoprecipitated together with syntaxins[23]. No evidence for its presence was found, although it cannot be excluded. Of three peptides sequenced, two were from Hsp70, an ATP-binding protein[28], and one was from a protein not found in the Genbank database.

Scanning and integrating the Coomassie blue stain in the gel shown in Fig. 2*a* gives the following ratios when staining is corrected for molecular weight, expressed as a fraction of α-SNAP: syntaxin B, 0.18; SNAP-25, 0.15; VAMP/synaptobrevin-2, 0.23. The syntaxin A band (band C) is weak compared with syntaxin B and could not readily be quantitated. The sum of all of the SNAP receptor species is 0.56 mol per mol α-SNAP, and so is approximately stoichiometric, given that proteins vary in staining by Coomassie blue, and the stoichiometry of SNAP and receptor in complexes does not need to be 1:1. The relative amounts of the different SNAP receptors in such a co-purified mixture may not reflect their relative abundance in the starting material, as their affinities for SNAPs may differ. The ratio of γ-SNAP to α-SNAP was ~0.2.

The role of syntaxins, SNAP-25, and synaptobrevin as SNAP receptors is supported by (1) their absence when NSF was omitted from the purification; (2) the need for ATP hydrolysis,

rather than the mere presence of ATP, to elute them from the beads; (3) the approximately stoichiometric amounts purified relative to SNAP itself; and (4) the substantial purity of the proteins obtained. The fact that all of these proteins originate from the synapse further strengthens this conclusion.

As further confirmation, we attempted to follow the incorporation of α-SNAP receptor into 20S particles formed from crude extracts of bovine brain membranes using an antibody raised against a C-terminal peptide from SNAP-25. Detergent extract from salt-washed membranes was incubated with excess recombinant α- and γ-SNAPs with (Fig. 4*c*) or without (Fig. 4*b*) excess recombinant NSF, and the products were separated by velocity centrifugation in a linear glycerol gradient. In the absence of NSF, SNAP-25 sedimented at about 5S, but in its presence, almost all SNAP-25 cosedimented with NSF, α-SNAP, and γ-SNAP in the 20S particle (Fig. 4*d*). Assembly of NSF and SNAPs into the 20S particle required bovine brain membrane extract (Fig. 4*a*), as expected from earlier studies with Golgi membranes[18].

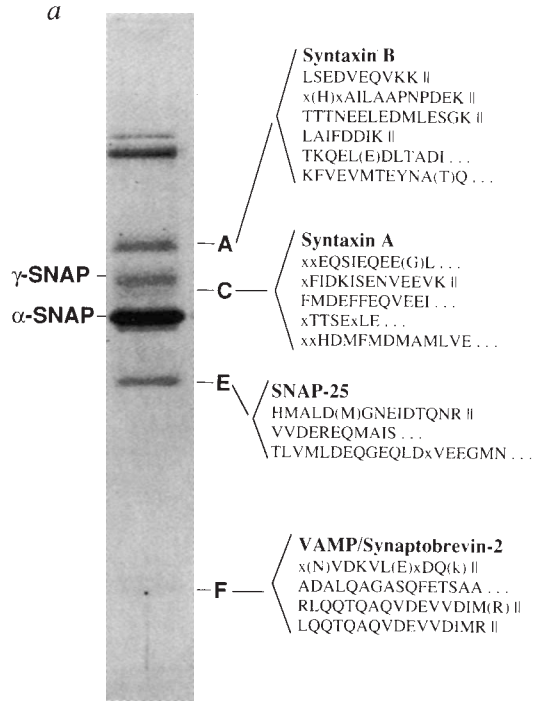

FIG. 3 Identification of SNAP receptors by amino-acid sequencing. Each of bands A–F was excised from an electroblot onto a nitrocellulose membrane after staining with Ponceau S, digested with trypsin, and the fragments separated by reverse-phase HPLC. *a*, Peptide sequences from each of the indicated bands are shown on the right (one-letter code). An 'X' means that no residue could be identified at this position. A capital letter in parentheses means that the residue was identified with a lower degree of confidence; a lower-case letter in parentheses means that the residue was present but in very small amounts. The symbol ‖ indicates that the C terminus of the peptide was known. A dotted line means no more interpretable signals were obtained, but that this was unlikely to be the C terminus. The identify of bands B and D (Fig. 2) as γ-SNAP and α-SNAP, respectively, was confirmed by peptide sequencing. In the case of the syntaxin A peptide XTTSExLE . . . (from band C), only this limited sequence was obtained because of instrument failure. However, mass analysis of this peptide (on 1/25th of the sample) gave a value of $m/z = 3{,}274.8$; this is in good agreement with the value ($MH^+ = 3{,}276.67$) calculated for the predicted tryptic peptide (residues 156–186 of syntaxin A) which contains the limited sequence, so confirming the identify of the entire peptide. Mass analysis was also critical in the identification of band F as VAMP/synaptobrevin-2, confirming the presence of an *N*-acetylated peptide corresponding to residues 2–31 in the digest of band F (see text for details). *b*, Amino-acid sequences of syntaxins A (top) and B (below) from rat brain[23]. Shown above syntaxin A are the peptide sequences obtained from band C, and below syntaxin B are the peptide sequences obtained from band A. *c*, Complete amino-acid sequence of synaptosome-associated protein 25 (SNAP-25) from mouse brain[24]. Above are the peptide sequences obtained from band E. Underlined sequences in *d* and *b* are peptides identified by mass analysis.

METHODS. Tryptic digestions and peptide separation. Ponceau S staining bands were excised, digested in situ with trypsin (1 μg sequencing grade trypsin; Boehringer-Mannheim), and the resulting fragments separated by RP-HPLC (ref. 50). Generally, HPLC systems were as described[50] and equipped with a 2.1 × 250 mm Vydac C4 (214TP54) column from the Separations Group (Hesperia, CA). Peptides resulting from digests of band F were fractionated on a 1 × 100 mm Inertsil 100GL-I-ODS-110/5 C18 column from SGE (Ringwood, Australia). The 1-mm column was operated in a system consisting of a model 140B syringe pump (ABI, Foster City, CA) and an ABI model 783 detector, fitted with a LC-Packings Kratos-compatible capillary flow cell which was directly connected to the column outlet (system assembly by C. Elicone); gradient slope was 1% B per min at a flow of 30 μl min^{-1}. Fractions were stored at −70 °C before sequence or mass analysis. Peptide sequencing: Peptides were sequenced with the aid of an ABI model 477A automated sequencer, optimized for femtomol phenylthiohydantoin analysis as described[51,52]. Fractions were always acidified (20% TFA final concentration) before application on the sequencer disc. Mass analysis: Aliquots (typically 1/50–1/25) of selected peak fractions were analysed by matrix-assisted laser desorption time-of-flight mass spectrometry using a Vestec (Houston, TX) LaserTec instrument with a 337 nm output nitrogen laser operated according to ref. 53. The matrix was α-cyano-4-hydroxy cinnamic acid and a 25 kV ion acceleration and 3 kV multiplier voltage were used. Laser power was adjusted manually as judged from optimal deflections of specific maxima, using a Tektronix TDA 520 digitizing oscilloscope.

Discussion

In this study, we have purified SNAP receptors from a crude brain membrane fraction on the basis of their ability to assemble

b

```
                                                FM DEFFEQVEEI   FIDKISEN
Rat Syntaxin A ---RTQELRT AKDSDDDDDV TVTVDRDRFM DEFFEQVEEI RGFIDKIAEN   47
Rat Syntaxin B MKDRTQELRS AKDSDDEEEV -VHVDRDHFM DEFFEQVEEI RGCIEKLSED   49
                                                                  LSED

            VEEVK                                                 EQSI
            VEEVKRKHSA ILASPNPDEK TKEELEELMS DIKKTANKVR SKLKSIEQSI      97
            VEQVKKQHSA ILAAPNPDEK TKQELEDLTA DIKKTANKVR SKLKAIEQSI      99
            VEQVKKxHxA ILAAPNPDEK TKQELEDLTA DI

            EQEEGL
            EQEEGLNRSS ADLRIRKTQH STLSRKFVEV MSEYNATQSD YRERCKGRIQ     147
            EQEEGLNRSS ADLRIRKTQH STLSRKFVEV MTEYNATQSK YRDRCKDRIQ     149
                                     KFVEV MTEYNATQ

                    T TSExLE
            RQLEITGRTT TSEELEDMLE SGNPAIFASG IIMDSSISKQ ALSEIETRHS     197
            RQLEITGRTT TNEELEDMLE SGKLAIFTDD IKMDSQMTKQ ALNEIETRHN     199
                    TT TNEELEDMLE SGKLAIFTDD IK

                       HDMFMDMA MLVE
            EIIKLENSIR ELHDMFMDMA MLVESQGEMI DRIEYNVEHA VDYVERAVSD     247
            EIIKLETSIR ELHDMFVDMA MLVESQGEMI DRIEYNVEHS VDYVERAVSD     249


            TKKAVKYQSK ARRKKIMIII CCVILGIIIA STIGGIFG-      285
            TKKAVKYQSK ARRKKIMIII CCVVLGVVLA SSIGGTLGL      288
```

c

```
Mouse SNAP-25
                                                    TLVML DEQGEQLDxV
        MAEDADMRNE LEEMQRRADQ LADESLESTR RMLQLVEESK DAGIRTLVML DEQGEQLERI  60

        EEGMN                                                        V
        EEGMDQINKD MKEAEKNLTD LGKFCGLCVC PCNKLKSSDA YKKAWGNNQD GVVASQPARV 120

        VDEREQMAIS                                  HMALDMGNE IDTQNR
        VDEREQMAIS GGFIRRVTND ARENEMDENL EQVSGIIGNL RHMALDMGNE IDTQNRQIDR 180


        IMEKADSNKT RIDEANQRAT KMLGSG  206
```

d

```
Bovine
VAMP/Synaptobrevin 2
                                    RLQQTQAQVD EVVDIMR NV DKVLExDQk
        MSATAATAPP AAPAGEGGPP APPPNLTSNR RLQQTQAQVD EVVDIMRVNV DKVLERDQKL  60

             ADAL QAGASQFET SAA
        SELDDRADAL QAGASQFET SAAKLKRKYW WKNLKMMIIL GVICAIILII IIVYFSS      117
```

20S particles from SNAPs and NSF, and their release from NSF upon ATP hydrolysis (studies using Golgi membranes as source material will be described elsewhere). The simplest explanation for the fact that multiple polypeptides are obtained is that each is a distinct SNAP receptor. In particular, there is no evidence that any of these polypeptides associate, for example, as heterodimers[54]. All of them must thus have either the capacity to assemble a 20S particle, or a very high affinity for one that has been assembled. As our method is biased to isolating receptors of the highest abundance and affinity, we have probably isolated only some of the receptor types that are present.

By exploiting the same enzyme cycle used in the vesicle fusion process to offer two layers of biological specificity, we have purified SNAP receptors on the basis of their function, giving a largely pure preparation of four proteins from the crudest possible extract of brain, all of which originate from synapses. This striking selection for synaptic components probably reflects the degree to which the brain is specialized for synaptic vesicle fusion. The fact that each SNAP receptor purified corresponds to a previously cloned and sequenced gene no doubt reflects the exhaustive structural characterization of synaptic components by molecular biologists who have focused on the synapse because of its central importance in neuronal development and function[29,30,54]. Despite this effort, however, the roles of these proteins are unknown because of the lack of functional assays.

Of the SNAP receptors we have isolated, SNAP-25 is found in the presynaptic terminals of neurons[24] but has not been more precisely localized. Although its sequence suggests it is hydrophilic, it behaves as an integral membrane protein[24] and is palmitylated at one or more of the four cysteine residues between positions 85 and 92 (ref. 55). Fatty acyl-CoA is required for NSF-dependent fusion[56], and SNAP-25 or related proteins may serve as the relevant acyl acceptors. Multiple acylations of such proteins could create a hydrophobic surface as a trigger for fusion.

VAMP/synaptobrevin is inserted into synaptic vesicles by a single hydrophobic C-terminal segment, and the remainder of the protein is cytoplasmic. Both tetanus and botulinum B toxins, potent inhibitors of neurotransmitter release, are proteases specific for VAMP/synaptobrevin-2 (ref. 31), suggesting that this SNAP receptor is essential for synaptic vesicle fusion *in vivo*. Syntaxin[23] has the same topography as VAMP/synaptobrevin, but is concentrated in 'active zones' of the presynaptic membrane[23] at which a subpopulation of synaptic vesicles is docked[32] to allow fusion within 200 μs of the calcium influx induced by an action potential[33]. Components of the fusion machinery may have to be largely preassembled at these sites to allow such a rapid response.

In this light, the fact that 20S particles can contain VAMP/synaptobrevin (from the synaptic vesicle) and syntaxin (from the plasma membrane) is of interest, because these complexes might form part of the fusion apparatus docking the vesicle to its target in the active zone. It is not yet possible to say whether syntaxin and VAMP/synaptobrevin exist together in a single 20S particle (Fig. 5*a*), or whether separately assembled particles join together to form an attachment site (Fig. 5*b*), perhaps with the aid of additional proteins.

The fact that molecules previously implicated in regulated exocytosis at the synapse are SNAP receptors implies that the same NSF- and SNAP-dependent machinery necessary for many constitutive fusion events also underlies triggered release of neutotransmitters at synapses. By extension, we would expect that NSF and SNAP are similarly employed in other forms of regulated exocytosis[34].

How can constititutive fusion machinery also be used in triggered exocytosis? An inhibitory component(s) must apparently prevent the 20S fusion particle from engaging, or from completely assembling in the first place. Such a fusion clamp could either cover an active site in NSF, SNAP or the SNAP receptors, or could prevent any of the additional cytoplasmic subunits of the fusion machinery[35] from binding. In the case of the synapse, a calcium trigger would remove the clamp. A strong candidate for such a clamp is the synaptic vesicle membrane protein synaptotagmin[36,37]. Synaptotagmin co-immunoprecipitates with syntaxin[23], and the recombinant pro-

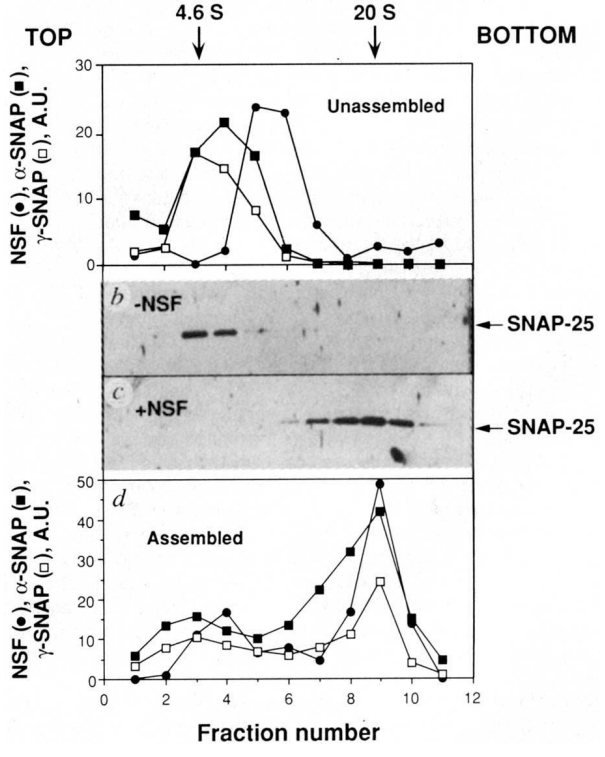

FIG. 4 Incorporation of SNAP-25 and other components into 20S fusion particles. *a*, *b*, Conditions in which 20S particles do not form (for example, controls); *c*, *d*, conditions in which 20S particles assemble. Components of the 20S fusion particle were incubated and then fractionated by glycerol gradient centrifugation, and the fractions analysed by SDS–PAGE to determine the location of α-SNAP and γ-SNAP, and to determine the locations of NSF and SNAP-25. Bovine serum albumin (4.6S) and α_2-macroglobulin (20S) were used as standards.

METHODS. Reaction conditions were arranged so that the protein of interest would be maximally incorporated into 20S particles; thus, results in *a* and *d* are composites of several experiments. In the case in which the SNAPs were examined, *in vitro*-translated ^{35}S-labelled α-SNAP (■) and γ-SNAP (□) (ref. 17) (~2.1×10^6 c.p.m. for α- and 1.4×10^5 c.p.m. for γ-SNAP) were incubated on ice with bovine brain extract (1.2 mg protein), in the absence (*a*) or presence (*d*) of His_6-NSF (100 μg protein) in 20 mM HEPES–KOH, pH 7.4, 100 mM KCl, 2 mM DTT, 2 mM EDTA, 0.5 mM ATP, 0.5% (v/v) Triton X-100 in a final volume of 0.5 ml. After 15 min, reactions were loaded onto a 10–35% (w/v) glycerol gradient[18] and centrifuged in an SW41 rotor (Beckman) for 18 h at 40,000 r.p.m. Gradients were fractionated from the bottom at 1 ml per min, and an aliquot of each fraction analysed by SDS–PAGE and autofluorography. Recovery of both radiolabelled SNAPs exceeded 90%. Autofluorographs were scanned with a ScanJet Plus (Hewlett Packard) and the images integrated using Scan Analysis software (BioSoft, Cambridge). To examine NSF (●), His_6-NSF (ref. 15) (10 μg protein) was incubated with each of the His_6-SNAPs (20 μg each protein), either in the absence (*a*) or presence (*d*) of bovine brain extract (1.5 mg protein). Samples were incubated and fractionated as described. Aliquots were analysed by western blotting using an anti-His_6 antibody and blots were scanned as described[17]. To determine the extent to which SNAP-25 is incorporated into the 20S particle, bovine brain extract was added in limiting amounts (300 μg protein) and incubated either in the absence (*b*) or presence (*c*) of both His_6-SNAPs and His_6-NSF (30 μg each protein). Samples were processed and aliquots of each fraction analysed by western blotting using an antibody generated against the C-terminal peptide of SNAP-25. For this purpose, a peptide of the sequence used in ref. 24 was synthesized but with an additional cysteine at the N terminus, and affinity-purified antibodies generated. Blots were visualized using the ECL System (Amersham). AU, arbitrary unit.

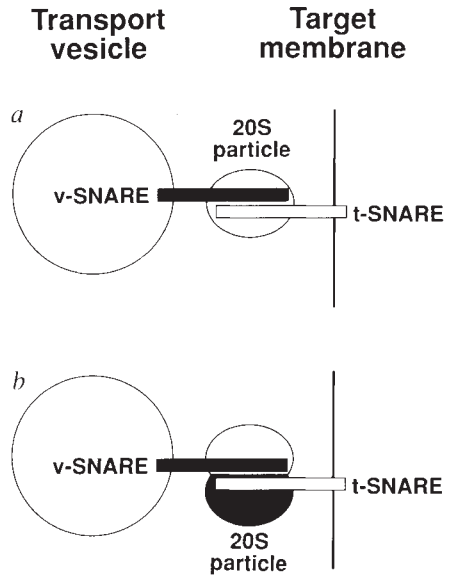

FIG. 5 Models to explain vesicle targeting based on the finding that SNAREs isolated in 20S fusion particles can originate from either the transport vesicle (v-SNAREs) or from the target membrane (t-SNAREs). A 20S particle (containing NSF and SNAPs) that simultaneously binds a v-SNARE and a t-SNARE (*a*) would attach a vesicle to its target. Alternatively (*b*), 20S particles, each capable of binding only one SNARE at a time, could interact to attach vesicle to target, a process that perhaps requires other proteins to assemble together.

teins can bind each other[23]. It also undergoes a calcium-dependent conformational change[38]. Although synaptotagmin is not one of the major components of the 20S particles characterized here, this is not surprising, as the interaction between syntaxin and synaptotagmin is disrupted by 0.5 M salt[23], and we used a 1 M salt wash.

Rab3A, a Ras-related GTP-binding protein, is another candidate for a clamp, as this protein dissociates from synaptic vesicles upon stimulation of fusion[39]. Fusion clamps may respond to a variety of second messengers such as cyclic AMP, activated G proteins, protein phosphorylation, and so on, in addition to calcium, depending on cell type and physiological context.

SNAREs may encode specificity

Both syntaxin and VAMP/synaptobrevin have homologues in yeast[40,42]. The yeast protein SED5 is related to syntaxin[40], and its absence blocks ER-to-Golgi transport, leading to the accumulation of transport vesicles; it appears to reside in the Golgi[40]. Another homologue, PEP12, is found primarily on the vacuole membrane, and is required for Golgi-to-vacuole transport[41]. The yeast *SEC22*, *BET1* and *BOS1* gene products are related to VAMP/synaptobrevin, and are required for fusion with the Golgi *in vivo*. BOS1 at least is a component of ER-derived transport vesicles[16,42-45]. Other recent examples are discussed in ref. 46. SNAP-25 is distantly related to SED5, PEP12, and the syntaxins.

The synaptic SNAP receptors we have identified are thus members of a family of proteins which appear to be distributed in a compartmentally specific fashion, with one set attached to the transport vesicles (v-SNAREs) and another set attached to target membranes (t-SNAREs). This suggests a model in which each transport vesicle contains one or more members of the v-SNARE superfamily obtained on budding from a corresponding donor compartment, and every target compartment in a cell contains one or more members of the t-SNARE superfamily. Specificity in membrane transactions would be assured by the unique and non-overlapping distribution of v-SNAREs and tSNAREs among the different vesicles and target compartments. In the simplest view, that is, if there were no other source of specificity, only when complementary v-SNARE and t-SNARE pairs engage would a productive fusion event be initiated. Thus, a v-SNARE from the ER (possibly SEC22) could engage a t-SNARE from the Golgi (possibly SED5), but not one from the lysosome (possibly PEP12). For the proposed mechanism to work (again, assuming no other source of specificity), non-complementary SNAREs would have to be excluded from the same 20S particle (Fig. 5*a*) or multi-particle assemblies (Fig. 5b), although any one SNARE might be able to form a 20S particle by itself while waiting for a partner to arrive. If this is correct, the 20S fusion particle assembly reaction might be used as a cell-free 'read-out' system to test whether candidate proteins are SNAREs (as shown here for SNAP-25), and to establish which SNAREs, if any, form specific cognate pairs. Localization of the SNARE proteins *in situ* would then establish which are v-SNAREs and which are t-SNAREs and which compartments are involved in each pairing.

A related mechanistic question is whether the SNAPs (and NSF) are associated primarily with a v-SNARE or with a t-SNARE, or whether an essentially symmetrical structure is formed at the junction of vesicle and target. NSF and SNAPs can associate with Golgi membranes to form 20S particles in the absence of transport vesicles[18], implying that 20S particles can be formed with only one SNARE partner. As native NSF is a tetramer of subunits with two ATPase domains each, it is easy to imagine several ways in which a 20S particle containing one NSF could form a symmetrical vesicle-target junction by simultaneously binding a v-SNARE and a t-SNARE (Fig. 5*a*).

Although many important details need to be established, our findings imply a general role for NSF and SNAP in regulated and constitutive intracellular membrane fusion processes, and in synaptic transmission in particular. The SNAREs we have identified appear to be members of compartment-specific membrane protein mutigene families which may form attachment sites between specific vesicles and their correct target membranes together with NSF and SNAPs. □

Received 25 February; accepted 9 March 1993.

1. Palade, G. E. *Science* **189,** 347-358 (1975).
2. Glick, B. S. & Rothman, J. E. *Nature* **326,** 309-312 (1987).
3. Block, M. R., Glick, B. S., Wilcox, C. A., Wieland, F. T. & Rothman, J. E. *Proc. natn. Acad. Sci. U.S.A.* **85,** 7852-7856 (1988).
4. Fries, E. & Rothman, J. E. *Proc. natn. Acad. Sci. U.S.A.* **77,** 3870-3874 (1980).
5. Balch, W. E., Dunphy, D. W., Braell, W. A. & Rothman, J. E. *Cell* **39,** 405-416 (1984).
6. Malhotra, V., Orci, L., Glick, B. S., Block, M. R. & Rothman, J. E. *Cell* **54,** 221-227 (1988).
7. Orci, L., Malhotra, V., Amherdt, M., Serafini, T. & Rothman, J. E. *Cell* **56,** 357-368 (1989).
8. Wilson, D. W. *et al. Nature* **399,** 355-359 (1989).
9. Novick, P., Ferro, S. & Schekman, R. *Cell* **25,** 461-469 (1981).
10. Graham, T. R. & Emr, S. D. *J. Cell Biol.* **114,** 207-218 (1991).
11. Weidman, P. J., Melancon, P., Block, M. R. & Rothman, J. E. *J. Cell Biol.* **108,** 1589-1596 (1989).
12. Clary, D. O. & Rothman, J. E. *J. biol. Chem.* **265,** 10109-10117 (1990).
13. Clary, D. O., Griff, I. C. & Rothman, J. E. *Cell* **61,** 709-721 (1990).
14. Griff, I. C., Schekman, R., Rothman, J. E. & Kaiser, C. A. *J. biol. Chem.* **267,** 12106-12115 (1992).
15. Whiteheart, S. W. *et al. Nature* **362,** 353-355 (1993).
16. Kaiser, C. A. & Schekman, R. *Cell* **61,** 723-733 (1990).
17. Whiteheart, S. W., Brunner, M., Wilson, D. W., Wiedmann, M. & Rothman, J. E. *J. biol. Chem.* **267,** 12239-12243 (1992).
18. Wilson, D. W., Whiteheart, S. W., Wiedman, M., Brunner, M. & Rothman, J. E. *J. Cell Biol.* **117,** 531-538 (1992).
19. Tagaya, M., Wilson, D. W. Brunner, M., Arango, N. & Rothman, J. E. *J. biol. Chem.* **269,** 2662-2666 (1993).
20. Munro, S. & Pelham, H. R. B. *Cell* **48,** 899-907 (1987).
21. Wilson, D. W. & Rothman, J. E. *Meth. Enzym.* **219,** 309-318 (1992).
22. Evan, G. I., Lewis, G. K., Ramsey, G. & Bishop, M. J. *Molec. cell. Biol.* **5,** 3610-3616 (1985).
23. Bennett, M. K., Calakos, N. & Scheller, R. H. *Science* **257,** 255-259 (1992).
24. Oyler, G. A. *et al. J. Cell Biol.* **109,** 3030-3052 (1989).
25. Sudhof, T. C. *et al. Neuron* **2,** 1475-1481 (1989).
26. Elferink, L. A., Trimble, W. S. & Scheller, R. H. *J. biol. Chem.* **264,** 11061-11064 (1989).
27. Archer, B. T., Ozcelik, T., Jahn, R., Franke, U. & Sudhof, T. C. *J. biol. Chem.* **265,** 17267-17273 (1990).
28. Chappell, T. G. *Cell* **45,** 3-13 (1986).
29. Greengard, P., Valturta, F., Czernik, A. J. & Benfenati, F. *Science* **259,** 780-785 (1993).
30. Trimble, W. S., Linial, M. & Sheller, R. H. *A. Rev. Neurosci.* **14,** 93-122 (1991).
31. Schiavo, G. *et al. Nature* **359,** 832-835 (1992).
32. Landis, D. M. D., Hall, A. K., Weinstein, L. A. & Reese, T. S. *Neuron* **1,** 201-209 (1988).
33. Llinas, R., Steinberg, I. Z. & Walton, K. *Biophys. J.* **33,** 323-352 (1981).
34. Kelley, R. B., *Science* **230,** 25-32 (1985).
35. Waters, R. G., Clary, D. O. & Rothman, J. E. *J. Cell Biol.* **118,** 1015-1026 (1992).
36. Perin, M. S., Fried, V. A., Mignery, G. A., Jahn, R. & Sudhof, T. C. *Nature* **34,** 260-263 (1990).
37. Wendland, B., Miller, K. G., Schilling, J. & Scheller, R. H. *Neuron* **6,** 993-1007 (1991).
38. Brose, N., Petrenko, A. G., Sudhof, T. C. & Jahn, R. *Science* **256,** 1021-1025 (1992).
39. Fischer von Mollard, G., Sudhof, T. C. & Jahn, R. *Nature* **349,** 79-81 (1991).
40. Hardwick, K. G. & Pelham, H. R. B. *J. Cell Biol.* **119,** 513-521 (1992).
41. Preston, R. A. *et al. Molec. cell. Biol.* **11,** 5801-5812 (1991).

42. Dascher, C., Ossig, R., Gallwitz, D. & Schmitt, H. D. *Molec. cell. Biol.* **11,** 872–885 (1991).
43. Newman, A. P., Groesch, M. E. & Ferro-Novick, S. *EMBO J.* **11,** 3609–3617 (1992).
44. Newman, A. P. *et al. Molec. cell. Biol.* **12,** 3663–3664 (1992).
45. Shim, J., Newman, A. P. & Ferro-Novick, S. *J. Cell Biol.* **113,** 55–64 (1991).
46. Bennett, M. K. & Scheller, R. H. *Proc. natn. Acad. Sci. U.S.A.* (in the press).
47. Harlow, E. & Lane, O. *Antibodies: A Laboratory Manual* (Cold Spring Harbor Laboratory Press, New York, 1988).
48. Laemmli, U. K. *Nature* **227,** 680–685 (1970).
49. Schlenstedt, G., Gudmundsson, G. H., Boman, H. G. & Zimmermann, R. *J. biol. Chem.* **265,** 13960–13968 (1990).
50. Tempst, P., Link, A. J., Riviere, L. R., Fleming, M. & Elicone, C. *Electrophoresis* **11,** 537–553 (1990).
51. Tempst, P. & Riviere, L. *Analyt. Biochem.* **183,** 290–300 (1989).
52. Erdjument-Bromage, H., Geromanos, S., Chodera, A. & Tempst, P. *Techniques in Protein Chemistry IV* (Academic, San Diego, in the press).
53. Beavis, R. C. & Chait, B. T. *Rapid Commun. Mass Spect.* **3,** 432–435 (1989).
54. Sudhof, T. C. & Jahn, R. *Neuron* **6,** 665–677 (1991).
55. Hess, D. T., Slater, T. M., Wilson, M. C. & Skene, J. H. P. *J. Neurosci.* **12,** 4634–4641 (1992).
56. Pfanner, N., Glick, B. S., Arden, S. R. & Rothman, J. E. *J. Cell Biol.* **110,** 955–961 (1990).

ACKNOWLEDGEMENTS. We thank M. Hum, L. Lacomis and M. Lui for help with protein digestions, HPLC separations and peptide sequencing; C. Elicone for custom assembly of the microbore HPLC system; M. Wiedmann for discussion; and W. Patton for gel scans and analysis. This work was supported by the Mathers Charitable Foundation, and by an NIH grant (to J.E.R.), a Fellowship of the Deutsche Forschungsgemeinschaft (to T.S.), a Fellowship from the Jane Coffin Childs Memorial Fund for Medical Research (to S.W.W.), and by an EMBO postdoctoral fellowship (to M.B.). The Sloan-Kettering microchemistry core facility is supported, in part, by an NCI core grant.

LETTERS TO NATURE

A young source of optical emission from distant radio galaxies

F. Hammer*†, O. Le Fèvre*† & M. C. Angonin*

* Département d'Astrophysique Extragalactique et Cosmologie, Observatoire de Paris-Meudon, 92195 Meudon Cedex, France
† Canada-France-Hawaii Telescope Corporation, PO Box 1597, Kamuela, Hawaii 96743, USA

DISTANT radio galaxies provide valuable insights into the properties of the young Universe—they are the only known extended optical sources at high redshift and might represent an early stage in the formation and evolution of galaxies in general. This extended optical emission often has very complex morphologies, but the origin of the light is still unclear. Here we report spectroscopic observations for several distant radio galaxies ($0.75 \leqslant z \leqslant 1.1$) in which the rest-frame spectra exhibit featureless continua between 2,500 Å and 5,000 Å. We see no evidence for the break in the spectrum at 4,000 Å expected for an old stellar population[1–3], and suggest that young stars or scattered emissions from the active nuclei are responsible for most of the observed light. In either case, this implies that the source of the optical emission is comparable in age to the associated radio source, namely 10^7 years or less.

One of the keys to understanding the nature of distant radio galaxies is the study of their optical continuum, and multiple broad-band photometry has been extensively used to examine their spectral energy distribution, often in conjunction with stellar population synthesis models. Contamination from various sources, however, can hide the true properties, and obviously affects the interpretation of the data. For example, distant radio galaxies generally have very strong emission lines, which can contribute significantly to broad-band photometric measurements both at visible and near-infrared wavelengths[4,5] (equivalent widths larger than several hundred angstroms); foreground galaxies[6] and even galactic stars[7] can project on the lines of sight. This is especially true when the broad-band photometry is performed on high redshift radio galaxies whose physical origin is still unclear and for which the multiple broad-band photometric data are at least as well fitted by simple power laws. To circumvent the problems inherent in such photometry[6–8], our goal here is to test the stellar contribution to the optical emission of distant radio galaxies from deep spectroscopic data.

The most convincing (stellar) model was presented by Lilly[1] and developed by Rigler *et al.*[2]. It assumes that the red continuum emission is due to a symmetric giant elliptical galaxy which becomes dominant at observed infrared wavelengths, while the ultraviolet emission consists of a flat component responsible for the alignment with the radio axis. Rigler *et al.*[2] have called this interpretation the 'old star hypothesis', and named another stellar scheme developed by Chambers and Charlot[3] the 'range of ages model'. The latter assumes a significant contribution of red supergiant stars (asymptotic giant branch) to the initial mass function, and that the optical colours of distant radio galaxies are an indication of their ages. Both models are apparently compatible with the small scatter of the K-band-magnitude–redshift (K–z) diagram, and seem adequately to fit the multiple broad-band photometric properties of distant radio galaxies. With the blue and red populations contributing roughly equally to the flux at 4,000 Å (ref. 2) in the 'old star' hypothesis, the continuum should exhibit a 4,000 Å break (from the old stars (>1 Gyr)) with a slope flattening due to the contribution of the blue population. Similarly, the 'range of ages' model predicts a significant 4,000 Å break for all sources, and especially for the reddest ones. Another model, put forward by Bithell and Rees[9], assumes a single and extremely young stellar component for distant radio galaxies and expects spectral signatures from young stars between 3,500 and 4,500 Å.

We have obtained deep red spectroscopy of a sample of distant radio galaxies with redshifts larger than 0.7 (beyond which the alignment effect becomes significant), and smaller than 1.1 (beyond which features above 4,700 Å enter the infrared window). One can successfully extract spectra of galaxies with red-magnitude (R) = 21.5 with a signal to noise ratio (S/N) $\geqslant$ 10 around 9,000 Å on 4-m class telescopes in 3 hours, with an excellent uniformity of the sky correction (that is, an average pixel-to-pixel deviation less than 10% of the corrected $R = 21.5$ continuum, or less than 0.1% of the sky background (O.L.F., manuscript in preparation)). The ability to detect features in the continuum of faint galaxies beyond $z = 1$ was demonstrated from our spectroscopy of the quasar 3CR245 companion[10]. This is a radio-quiet galaxy at $z = 1.013$, which has optical magnitudes more than 1 mag less than distant 3CR galaxies (visible magnitude $V = 22.4$), and for which the 4,000 Å break and the Ca II, H and K bands are remarkably well detected in only two integrations of 45 min each ($S/N > 10$). The galaxy morphology and the amplitude of the break (D(4,000 Å) = 2; see Bruzual[11] for the definition) are characteristic of an elliptical galaxy, as is the detection of relatively strong absorption lines (Ca II, G band). For 3CR galaxies which have brighter magnitudes at optical wavelengths, one would therefore expect to identify spectral absorption features in the continuum in only a few hours of integration under similar observing conditions.

We observed 10 distant 3CR galaxies with redshifts ranging from 0.75 to 1.1. Their optical emission is aligned within 30° of the radio axis, and their infrared–visual colours range from R-K = 2.5 to 4, typical of distant radio galaxies. Some of our objects are red enough to be classified by Chambers and Charlot[3] as older galaxies ($\geqslant$1 Gyr), and although we miss some of the reddest objects such as 3CR65, we expect this sample adequately to describe the properties of most of the $z > 0.7$ powerful radio galaxies. Figure 1 shows the spectra of 3CR54, 265 and 343.1, compared to the galaxy companion of 3C245 and the residual noise extracted from the two-dimensional data. The S/N on the continuum at 4,000 Å is 9, 8, 12, 12 for these four objects respectively. As can be seen in the examples in Fig. 1, despite

Neuron, Vol. 15, 663–673, September, 1995, Copyright © 1995 by Cell Press

Syntaxin and Synaptobrevin Function Downstream of Vesicle Docking in Drosophila

Kendal Broadie,*† Andreas Prokop,*† Hugo J. Bellen,‡ Cahir J. O'Kane,§ Karen L. Schulze,‡ and Sean T. Sweeney§
†Department of Zoology
§Department of Genetics
University of Cambridge
Cambridge CB2 3EJ
England
‡Howard Hughes Medical Institute
Division of Neuroscience
and Department of Molecular and Human Genetics
Baylor College of Medicine
Houston, Texas 77030

Summary

In synaptic transmission, vesicles are proposed to dock at presynaptic active zones by the association of synaptobrevin (v-SNARE) with syntaxin (t-SNARE). We test this hypothesis in Drosophila strains lacking neural synaptobrevin (n-synaptobrevin) or syntaxin. We showed previously that loss of either protein completely blocks synaptic transmission. Here, we attempt to establish the level of this blockade. Ultrastructurally, vesicles are still targeted to the presynaptic membrane and dock normally at specialized release sites. These vesicles are mature and functional since spontaneous vesicle fusion persists in the absence of n-synaptobrevin and since vesicle fusion is triggered by hyperosmotic saline in the absence of syntaxin. We conclude that the SNARE hypothesis cannot fully explain the role of these proteins in synaptic transmission. Instead, both proteins play distinct roles downstream of docking.

Introduction

The directed movement of molecules within and between cells depends on the precise targeting of transport vesicles to specific membrane compartments. The SNARE hypothesis proposes that this specificity is achieved through the mutual recognition of an integral vesicle protein (v-SNARE) and an integral target membrane protein (t-SNARE; Söllner et al., 1993a, 1993b; Bennett and Scheller, 1994; Jahn and Südhof, 1994). In synaptic transmission, transmitter vesicles are believed to be targeted to fusion sites in the presynaptic membrane by the association of a specific VAMP, neural synaptobrevin (n-synaptobrevin) (v-SNARE), with the target membrane protein syntaxin (t-SNARE; Söllner et al., 1993a, 1993b; Pevsner et al., 1994). The binding of these proteins is proposed to mediate vesicle "docking" at their specialized fusion sites, a prerequisite state for Ca^{2+}-dependent exocytosis.

*The first two authors contributed equally to this work.

In vivo tests of the SNARE hypothesis at the synapse have made use of clostridial neurotoxins, peptide fragments, and monoclonal antibodies as tools specifically to cleave or inhibit syntaxin and synaptobrevin (Blasi et al., 1993; Bennett et al., 1993; Niemann et al., 1994). Cleavage of syntaxin by injection of botulinum neurotoxin C1 into squid synapses (Blasi et al., 1993) or injection of syntaxin-1A (*syn-1A*) fragments or anti-syntaxin antibodies into PC12 cells both cause a depression of Ca^{2+}-dependent transmission (Bennett et al., 1993). Likewise, cleavage of synaptobrevin by injection of the tetanus neurotoxin into squid synapses decreases synaptic transmission (Hunt et al., 1994). Vesicles continue to cluster and dock at squid presynaptic active zones following tetanus injection (Hunt et al., 1994), suggesting that synaptobrevin may not be required for this process in the squid. However, the role of syntaxin in directed vesicle docking has not yet been tested.

In recent years the powerful genetics of Drosophila has provided tools to study the development and function of synapses (reviewed by Broadie, 1994, 1995). In Drosophila, there is a neurally expressed synaptobrevin gene, n-synaptobrevin, and a ubiquitously expressed homolog, synaptobrevin, suggesting that these proteins might be functional homologs of the vertebrate synaptobrevin and cellubrevin, respectively (Chen et al., 1993; DiAntonio et al., 1993). In addition, a single Drosophila syntaxin homolog has recently been identified that shows strong homology to rodent syn-1A (82% similar; Schulze et al., 1995). In this study, we make use of Drosophila strains lacking n-synaptobrevin or syntaxin to study the synaptic roles of these proteins. Previous studies (Schulze et al., 1995; Sweeney et al., 1995) have shown that both syntaxin and n-synaptobrevin are essential for evoked synaptic transmission in Drosophila. Here, we attempt to define the level of this activity blockade. We show at the ultrastructural level that neither n-synaptobrevin nor syntaxin is required to dock mature vesicles at presynaptic active zones. We show that while spontaneous vesicle fusion persists in the absence of n-synaptobrevin, it is eliminated in the absence of syntaxin. We show that loss of n-synaptobrevin or syntaxin blocks fusion in response to a Ca^{2+}-independent fusion signal (latrotoxin) but not to nonspecific fusion stimuli (hyperosmotic saline). These experiments suggest that both proteins function downstream of docking: syntaxin is required for all vesicle fusion at the synapse, whereas n-synaptobrevin is required only for Ca^{2+}-dependent fusion. We conclude that the simple SNARE hypothesis as currently formulated cannot fully explain vesicle targeting during synaptic transmission.

Results

Deletion of Syntaxin or n-Synaptobrevin Eliminates Synaptic Transmission

Both syntaxin and n-synaptobrevin are strongly expressed in the Drosophila nervous system, and, at maturity, both

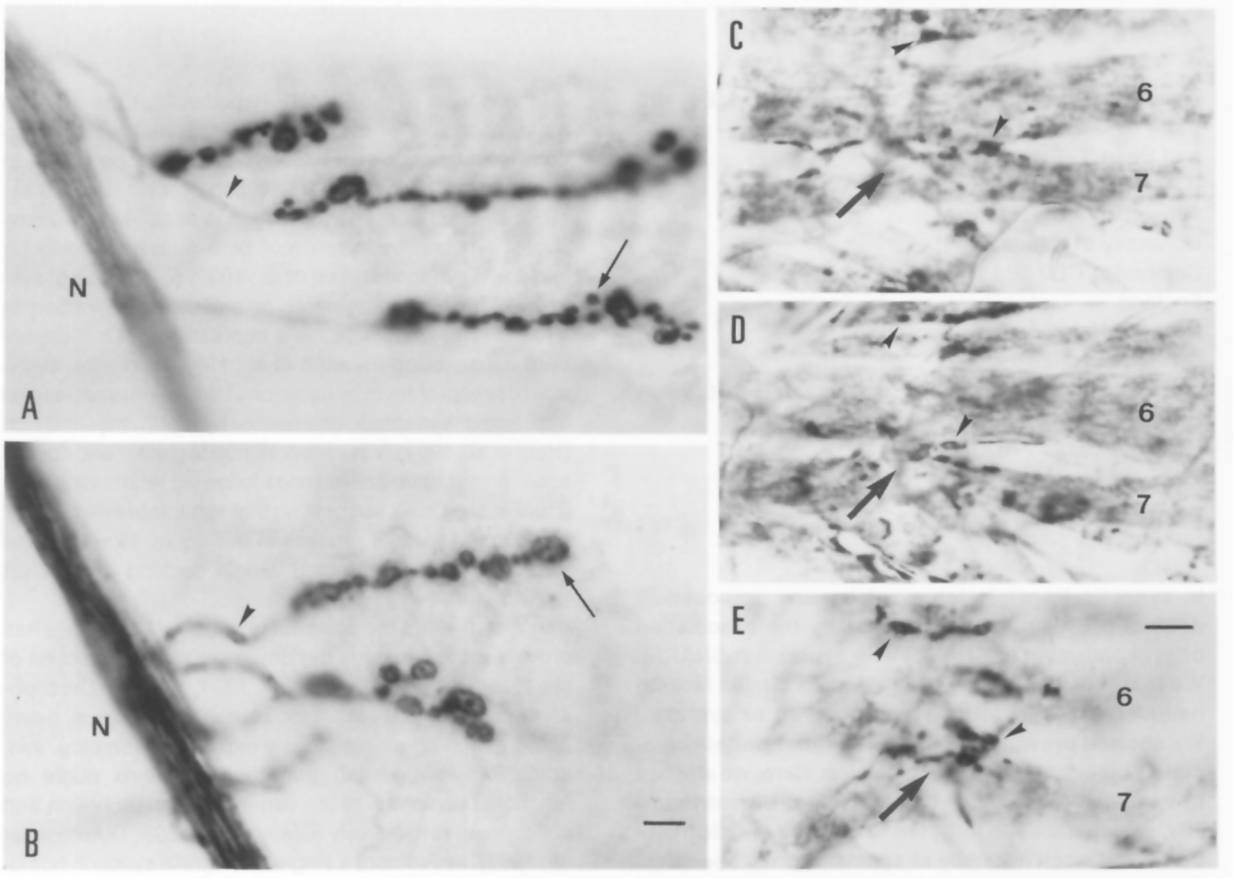

Figure 1. Syntaxin and n-Synaptobrevin Are Expressed in the Drosophila NMJ, but Are Not Required for Normal Synaptic Development

(A) The expression of n-synaptobrevin in the mature larval NMJ. The protein is strongly expressed in synaptic boutons (arrow), the sites of presynaptic active zones, but absent, or at very low levels, in the motor axon (arrowhead) and peripheral motor nerve (N).

(B) Syntaxin is strongly expressed in synaptic boutons (arrow) and also in individual motor axons (arrowhead) and a large number of axons within the peripheral nerve (N).

(C–E) Mature embryonic synaptic morphology at the muscle 6/7 NMJ (arrows) in wild type (C), TNT (D), and *syx* (E) embryos stained for the integral vesicle protein synaptotagmin. The NMJ morphology and synaptic boutons (arrowheads) are indistinguishable in wild type (C) and TNT (D). In *syx* (E) the NMJ occupies its normal domain and contains normal boutons (arrowhead), though, on average, the number of boutons is reduced 30%–50% relative to normal.

Scale bar, 5 μm.

proteins are highly enriched at neuromuscular junction (NMJ) boutons (Figures 1A and 1B). Synaptobrevin is largely restricted to these sites of vesicle release and shows only low levels of expression in the motor axons (Figure 1A). Likewise, syntaxin is enriched in synaptic boutons, but is also expressed at high levels throughout the axons of the peripheral nerves (Figure 1B). Thus, while both syntaxin and n-synaptobrevin proteins are present in presynaptic boutons, only n-synaptobrevin shows significantly restricted expression to these sites (Figure 1). The dispersed expression of syntaxin contrasts strongly with the localized expression of other synaptic proteins such as synaptotagmin (Broadie et al., 1994) and cysteine string protein (Zinsmaier et al., 1990).

Recently, we have removed syntaxin or n-synaptobrevin from Drosophila using distinct genetic approaches (see Experimental Procedures; Schulze et al., 1995; Sweeney et al., 1995). Deletion of either protein results in paralysis and embryonic lethality, and evoked synaptic transmission is completely eliminated at the NMJ (Figure 2). However, in the absence of either protein, the postsynaptic membrane responds normally to the applied neurotransmitter, L-glutamate, indicating that transmitter receptors cluster normally in the postsynaptic membrane (Figure 2). These observations suggest that both n-synaptobrevin and syntaxin may be required for the presynaptic release of transmitter vesicles. In the following, we analyzed mature embryonic NMJs in syntaxin null mutants (*syx*) and embryos lacking n-synaptobrevin due to the transgenic expression of TNT with various techniques to determine in which transmission step n-synaptobrevin and syntaxin proteins are required.

Mature Synapses Develop in the Absence of Either Syntaxin or n-Synaptobrevin

The loss of syntaxin or n-synaptobrevin might lead to a number of presynaptic defects. One possibility is that these proteins are required for synaptic development. However, in the absence of either protein, NMJs develop in the normal synaptic domain of target muscles and differ-

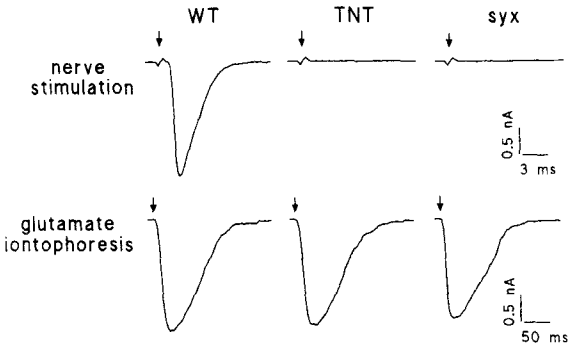

Figure 2. Deletion of Either n-Synaptobrevin or Syntaxin Completely Eliminates Synaptic Transmission at the Drosophila NMJ

The upper traces show nerve stimulation with a suction electrode and record the resulting synaptic current in the voltage-clamped muscle. All records were made in mature embryos (22–24 hr AEL) from muscle 6. In wild-type (WT) embryos, a robust synaptic current is observed, whereas in TNT-expressing embryos or syntaxin null mutant (*syx*) embryos, the evoked synaptic current is abolished. In all three genotypes, the postsynaptic muscle membrane responds normally to the iontophoretically applied transmitter L-glutamate, indicating that a normal postsynaptic receptive field is present and functional. Thus, both n-synaptobrevin and syntaxin are essential components of the presynaptic signaling machinery.

entiate boutons that are indistinguishable from wild type at the light microscope level (see Figures 1C–1E). TNT embryos show completely normal NMJs with the wild-type number and distribution of synaptic boutons (see Figure 1D), whereas the number of boutons is reduced on average by 30%–50% in *syx* mutants (see Figure 1E). The reduction of synaptic boutons in *syx* would be predicted to attenuate the evoked synaptic current but could not explain its complete elimination (Figure 2).

Besides morphological criteria, we tested TNT and *syx* for subcellular components by making use of existing antibodies. The transmitter L-glutamate accumulates at high concentrations in presynaptic boutons of *syx* and TNT and is indistinguishable from wild type (data not shown). Likewise, cysteine string protein, synaptotagmin, syntaxin (in TNT), and n-synaptobrevin (in *syx*) are expressed in the normal abundance and distribution in the absence of either syntaxin or n-synaptobrevin (synaptotagmin localization shown in Figures 1C–1E). Thus, the synapse accumulates the normal presynaptic proteins involved in evoked vesicle fusion. We conclude that defective synapse development, the absence of presynaptic transmitter, or the loss of other known components of the presynaptic vesicle release machinery does not explain the syntaxin or n-synaptobrevin mutant phenotypes.

Vesicles Dock at Active Zones in the Absence of Syntaxin or n-Synaptobrevin

Synaptic vesicles are normally docked at specialized release sites at the presynaptic membrane in preparation for evoked fusion (Kelly, 1993). According to the SNARE hypothesis, removal of either n-synaptobrevin or syntaxin from the synapse should block the targeted docking of vesicles to the presynaptic membrane (Pevsner et al., 1994). Such a block would be expected to eliminate synaptic transmission and so might explain the Drosophila mutant phenotypes. To test for this possibility, we analyzed wild-type, *syx*, and TNT NMJs at the ultrastructural level.

Most NMJs in the Drosophila embryo contain boutons with specialized presynaptic densities, so called t-bars (Osborne, 1975), which most likely correspond to the type I boutons described for the larva (Johansen et al., 1989). This is the only bouton type present at the NMJ of muscles 6 and 7 (Atwood et al., 1993; Jia et al., 1993), the synapse we used for our electrophysiological studies (see Figure 1C). At late larval stages, type I boutons are embedded in the muscle tissue and completely surrounded by reticular muscle specializations, the subsynaptic reticulum (e.g., Osborne, 1967; Lahey et al., 1994). In the late wild-type embryo, such boutons are only half embedded in the muscle tissue, and the other half is covered with basement membrane. Subsynaptic reticulum is not yet detectable, although occasional simple tubular invaginations of the muscle membrane can be observed (data not shown). Vesicles in such boutons are mostly translucent, are 30–40 nm in diameter, and are concentrated in a cloud surrounding the electron opaque t-bars (Figure 3). These t-bars are composed of a stem, about 50 nm in height, separated from a bar-like roof by a very narrow gap. The pre- and postsynaptic membranes underlying these t-bars appear smooth and electron dense over a stretch of several hundred nanometers and are separated by a very regular cleft of 15 nm. Only in these regions a line of electron opaque material can be detected in the cleft, more closely associated with the postsynaptic membrane (for discussion see Osborne, 1975). Such t-bar areas are identical in size and appearance to larval sites in Drosophila (e.g., Atwood et al., 1993; A. P., unpublished data) and are believed to be the vesicle release sites comparable to active zones in vertebrate NMJs (Heuser and Reese, 1973; Osborne, 1975; Heuser et al., 1979; Probst and Ko, 1987; Govind et al., 1980; Jia et al., 1993). The presence of morphologically mature release sites in late embryos correlates with the finding that embryonic NMJs at this stage have mature electrophysiological properties (Broadie and Bate, 1993a, 1993b).

The ultrastructure of embryonic synapses in *syx* and TNT mutants was largely indistinguishable from wild type (Figure 3). In particular, all three genotypes showed localized clustering of clear synaptic vesicles at t-bar release sites in both the NMJ (Figure 3) and in the CNS (data not shown). When vesicles were counted within a range of 180 nm (5-vesicle diameters) from release sites, *syx* showed a comparable number of clustered vesicles to wild type (Table 1). In contrast, TNT release sites showed an approximately 50% increase in clustered vesicles, a highly significant increase over wild type (Table 1). In all three genotypes, vesicles were found in direct physical contact with the t-bar and the electron dense presynaptic membrane under the bar-like roof of t-bars (Figure 3), a position at which exocytotic figures were reported in the larva (Jia et al., 1993). In both *syx* and TNT, the percentage of clustered vesicles that contacted the membrane (or were distributed up to a vesicle diameter distant from the membrane) was

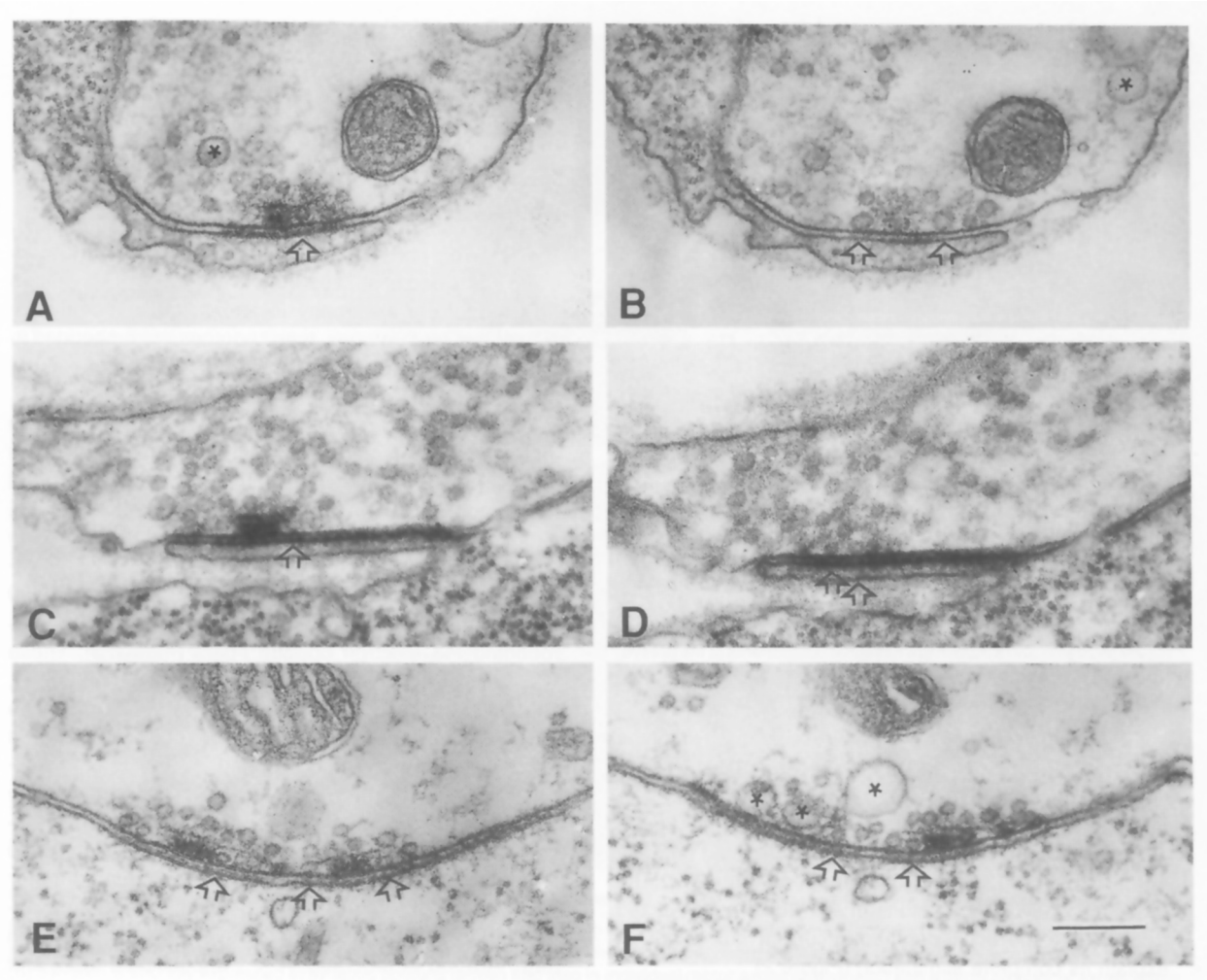

Figure 3. By Ultrastructural Criteria, Synaptic Vesicles Dock at Presynaptic Release Sites in the Absence of Either n-Synaptobrevin or Syntaxin

The left and right images represent sequential sections of the same release site, taken from embryonic wild-type (A and B), TNT (C and D), and *syx* (E and F) synapses. All release sites show the typical features (e.g., t-bars, electron dense membrane, synaptic cleft material) described in the text. In all three genotypes, vesicles directly contact the presynaptic membrane (open arrows) and appear docked. In all three genotypes, docked vesicles (open arrows) are located under the bar-like roof of release site t-bars, the position at which exocytotic figures were reported in the larva (Jia et al., 1993). Scale bar, 200 nm.

significantly increased compared with wild type (Table 1). According to ultrastructural criteria (see, e.g., Heuser et al., 1979; Bommert et al., 1993; Hess et al., 1993; Hunt et al., 1994; DeBello et al., 1995), we consider these vesicles to be docked. Thus, both vesicle clustering and docking at release sites occur normally in the absence of either syntaxin or n-synaptobrevin, and the number of docked vesicles is significantly increased in the absence of either protein.

In TNT embryos, both NMJs and central synapses ap-

Table 1. Vesicle Distribution of NMJ Release Site

			Clustered Vesicles per Micrometer				Percent Docked Vesicles			
				Sections		Mann–Whitney U Test Significance Related to Wild		Sections		Mann–Whitney U Test Significance Related to Wild
Embryos	Membrane (μm)	Number of Sections	Total	SD	SE	Type	Total	SD	SE	Type
Wild type	8.5	20	21.9	22.6 ± 8.3	1.9	—	18	17.8 ± 8.1	1.8	—
TNT	9.0	25	33.3	34.1 ± 7.8	1.6	$p < 0.001$	22	24.3 ± 12.8	2.6	$p < 0.05$
syx^{229}	11.8	18	20.3	20.9 ± 8.0	1.9	$p > 0.5$	28	28.3 ± 12.4	2.9	$p < 0.01$

The total length of release site membrane and number of analyzed independent sections are given for each genotype. Clustered vesicles are counted as those within 180 nm (5-vesicle diameters) of the release site. Docked vesicles are counted as those within 40 nm (< 1-vesicle diameter) of the release site. Significance was analyzed using the Mann–Whitney U test.

pear morphologically normal (Figures 3C and 3D). In *syx*, the only detectable morphological abnormality at the ultrastructural level was an unusual abundance of enlarged vesicles (>45 nm diameter) besides normal vesicles (Figures 3E and 3F). Among vesicles counted at release sites, 8% were enlarged in *syx* compared with 1% in wild type and 2% in TNT. These enlarged vesicles could be seen throughout the synapse but also in direct contact with the presynaptic membrane at t-bar release sites (Figures 3E and 3F). The same specific defect was detected in embryos mutant for the hypomorph allele P[*syx*] (27.4% ± 8.2% clustered vesicles per micrometer of membrane; 21.5% ± 8.4% docked, 7.6% enlarged), suggesting a primary role of *syx* in this phenotype. The significance of this defect is unclear but is clearly separable from the electrophysiological block since both evoked transmission and spontaneous release persist in P[*syx*] hypomorphs (Schulze et al., 1995).

Deletion of Syntaxin Eliminates Synaptic Vesicle Fusion

As the deletion of syntaxin or n-synaptobrevin still allows for proper docking of vesicles, we next asked whether these vesicles were also capable of fusing spontaneously to the presynaptic membrane. Like other synapses, the embryonic Drosophila NMJ shows spontaneous miniature excitatory junctional currents (MEJCs) in the absence of stimulation (Broadie et al., 1994; Kidikoro and Nishikawa, 1994). Such MEJCs are believed to result from the spontaneous fusion of synaptic vesicles with the presynaptic membrane. In the normal range of recording salines (1–2 mM Ca^{2+}), spontaneous MEJCs occur at a high frequency and multiquanta events are common, making analyses difficult (see Discussion). In the absence of external Ca^{2+}, the Ca^{2+}-dependent multiquanta events are largely eliminated (Broadie et al., 1994). However, two distinct classes of MEJCs are still observed (Figures 4A and 4C): rare class 1 MEJCs (<0.01 Hz), with a larger amplitude and rapid time course, and more common class 2 MEJCs (0.1 Hz), with a smaller amplitude and markedly slow time course. It appears that class 1 MEJCs represent quanta in the patch-clamped muscle and class 2 MEJCs represent quanta in adjacent, electrically coupled muscle fibers (see Discussion). In this analysis, we pool these two MEJC populations (Figure 4).

In TNT, both class 1 and 2 of MEJCs occur at the mature embryonic NMJ, though at a frequency approximately half that of wild type (Figures 4B and 4C; Sweeney et al., 1995). In contrast, in *syx* mutants, all MEJCs are essentially absent at the NMJ, though extremely rare fusion events are still observed (<0.005 Hz; Figure 4). Unlike TNT, *syx* mutants do not display any increase in MEJC frequency in the presence of external Ca^{2+} (Schulze et al., 1995; Sweeney et al., 1995). Though *syx* embryos failed to display MEJCs, they still showed clustered and docked vesicles at release sites when subsequently analyzed at the ultrastructural level (data not shown). These observations show that docked vesicles in TNT are functional and that n-synaptobrevin is not required for their spontaneous fu-

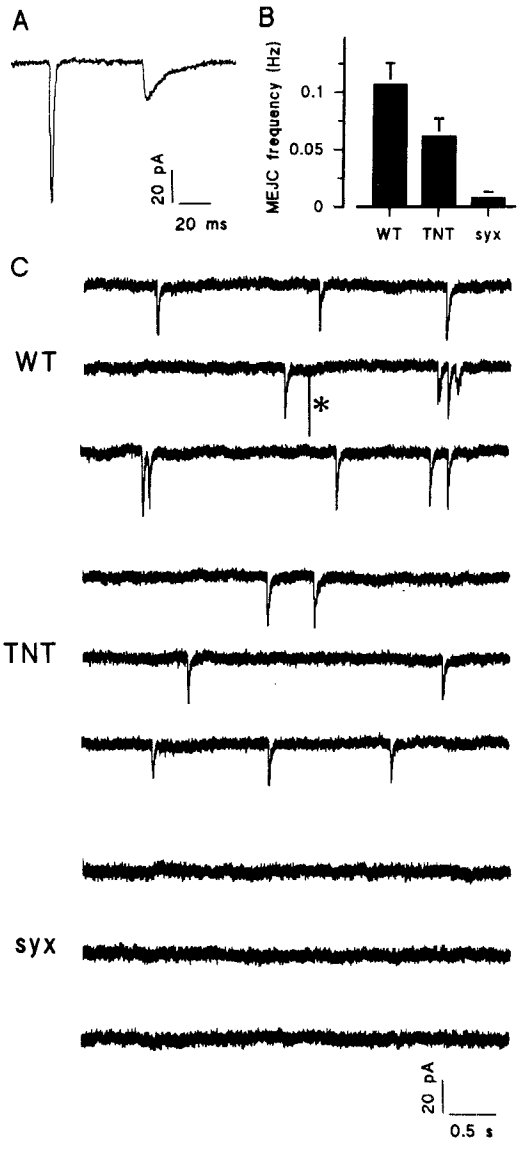

Figure 4. Spontaneous Vesicle Fusions Persist in NMJs Lacking n-Synaptobrevin but Are Absent in Synapses Lacking Syntaxin

(A) In wild-type embryos, two classes of MEJCs are recorded at the NMJ on muscle 6: class 1, with a larger amplitude and fast time course (left), and class 2, with a smaller amplitude and slower time course (right). Class 1 MEJCs are believed to arise from quanta released at the muscle 6 NMJ and class 2 MEJCs from quanta released on adjacent, coupled muscle fibers. Both populations are pooled in the following analyses.

(B) The frequency of MEJCS in wild type (WT), in the absence of synaptobrevin (TNT), and in syntaxin null mutants (*syx*). In TNT, MEJC frequency is reduced approximately 50% relative to WT. In *syx*, MEJCs are essentially absent. The results represent the mean ± SEM from at least 10 embryos of each genotype. All studies were carried out in 0 mM external Ca^{2+} to eliminate Ca^{2+}-dependent multiquanta events.

(C) Examples of MEJCs in wild type (WT), TNT, and *syx* in 0 mM external Ca^{2+}. In the wild-type trace, a rare class 1 MEJC (shown by asterisk) can be observed. Both classes of MEJCs can be seen in TNT synapses, whereas these events are never seen in *syx*.

sion, though it plays a small facilitory role. Syntaxin, however, plays a central role in spontaneous as well as evoked vesicle fusion.

A Ca^{2+}-Independent Fusion Signal, Latroinsectotoxin, Fails to Stimulate Vesicle Fusion in the Absence of Syntaxin or n-Synaptobrevin

To characterize further the regulatory level at which n-synaptobrevin and syntaxin are required, we studied the effect of known independent signals on transmission in TNT and *syx*. One such method is the application of black widow spider venom (BWSV) (Magazanik et al., 1992; Ramaswami et al., 1994). A component of BWSV, latroinsectotoxin, triggers both Ca^{2+}-dependent and Ca^{2+}-independent fusion of synaptic vesicles at insect NMJs that is independent of depolarization (Magazanik et al., 1992; Ramaswami et al., 1994; see Discussion). In mature embryonic NMJs, application of BWSV elicits high levels of synaptic vesicle fusion in the presence of external Ca^{2+} and a smaller, though still robust, vesicle fusion that is Ca^{2+}-independent (Figure 5A). Under Ca^{2+}-free conditions, BWSV application results in a 10-fold increase in MEJC frequency at the NMJ (Figure 5B). Ultrastructural analysis of embryos treated for 10 min with BWSV reveals normal clustering of vesicles at active zones (data not shown; see also Clark et al., 1970, 1972). Thus, there is no indication for the possibility that latrotoxin-induced release takes place at sites other than the presumptive active zones.

In TNT synapses, both the Ca^{2+}-dependent and Ca^{2+}-independent BWSV-induced vesicle fusion is blocked (Figures 5A and 5B). When BWSV is applied to the synapse, the spontaneous vesicle fusion rate continues unaltered (Figure 5A). Thus, both a depolarization-independent Ca^{2+} trigger and a separate Ca^{2+}-independent signal fail to trigger vesicle fusion in the absence of n-synaptobrevin. Likewise, in *syx* mutants, BWSV does not induce appreciable fusion rates in the presence or absence of external Ca^{2+} (Figure 5B). We conclude that both n-synaptobrevin and syntaxin are required for latrotoxin-induced fusion of synaptic vesicles.

Mature Synaptic Vesicles Are Present in the Absence of Syntaxin or n-Synaptobrevin

Another independent signal to trigger transmission is the application of hyperosmotic saline to presynaptic terminals. Hyperosmotic saline greatly increases MEJC frequency in a variety of neuromuscular preparations (Furshpan, 1956; Niles and Smith, 1982) and at central synapses (Bekkers and Stevens, 1989) due to release of the restricted pool of docked vesicles (Stevens and Tsujimoto, 1995). Similarly, in embryonic Drosophila NMJs, application of hyperosmotic bath saline induces a dramatic increase in MEJC frequency (Figure 6). A 50% increase in osmolarity (from 300 to 450 mOsm) results in a maintained 5- to 10-fold increase in MEJC frequency. Greater changes in osmolarity (from 300 to 600 mOsm) result in prolonged mass exocytosis of vesicles (Figure 6), which then decreases. Stimulation of the motor nerve over time (up to 1 hr) in such hyperosmotic solutions leads to progressively

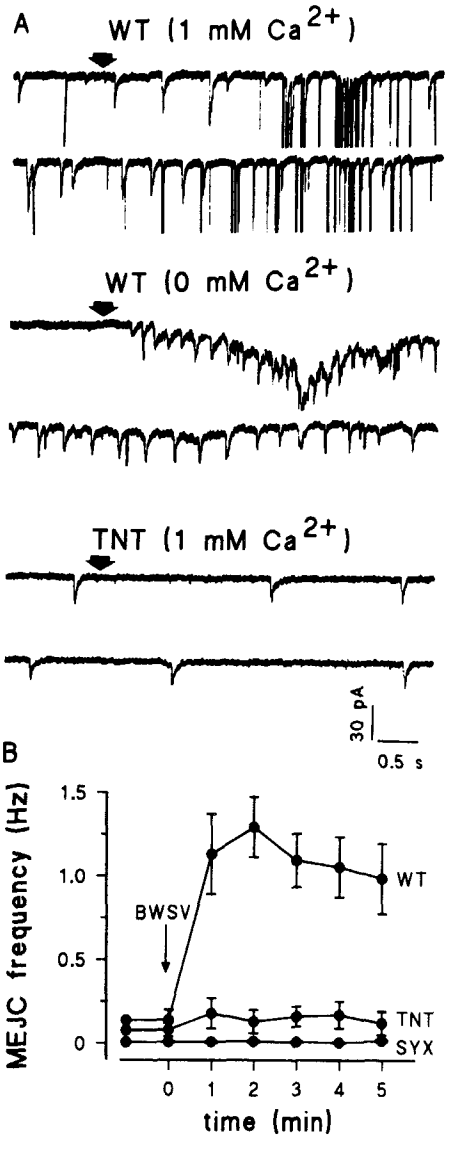

Figure 5. Latroinsectotoxin Does Not Stimulate Vesicle Fusion in the Absence of Syntaxin or n-Synaptobrevin

(A) In wild-type (WT) NMJs, BWSV application (arrows) induces the mass exocytosis of synaptic vesicles at the NMJ that has both Ca^{2+}-dependent (top trace) and Ca^{2+}-independent (middle trace) components. In the presence of external Ca^{2+} (1.0 mM; top trace), toxin application induces prolonged high frequency MEJCs and macroscopic synaptic currents (up to 500 pA). In the absence of Ca^{2+} (middle trace), toxin application induces prolonged release of high frequency MEJCs, but the macroscopic currents are absent. In TNT-expressing synapses, toxin application does not alter MEJC frequency either in the presence (1.0 mM Ca^{2+}) or absence of external Ca^{2+} (bottom trace). In *syx* mutants, appreciable rates of MEJCs are not stimulated by BWSV (data not shown).

(B) MEJC frequencies following application of BWSV in wild-type (WT), TNT-expressing, and syntaxin mutant (*syx*) NMJs in the absence of external Ca^{2+}. Each point shows the mean ± SEM from at least 10 trials.

reduced EJC amplitudes, suggesting that the number of available vesicles is being depleted (data not shown).

In TNT embryos, which have already been demonstrated to allow spontaneous MEJCs, application of hyper-

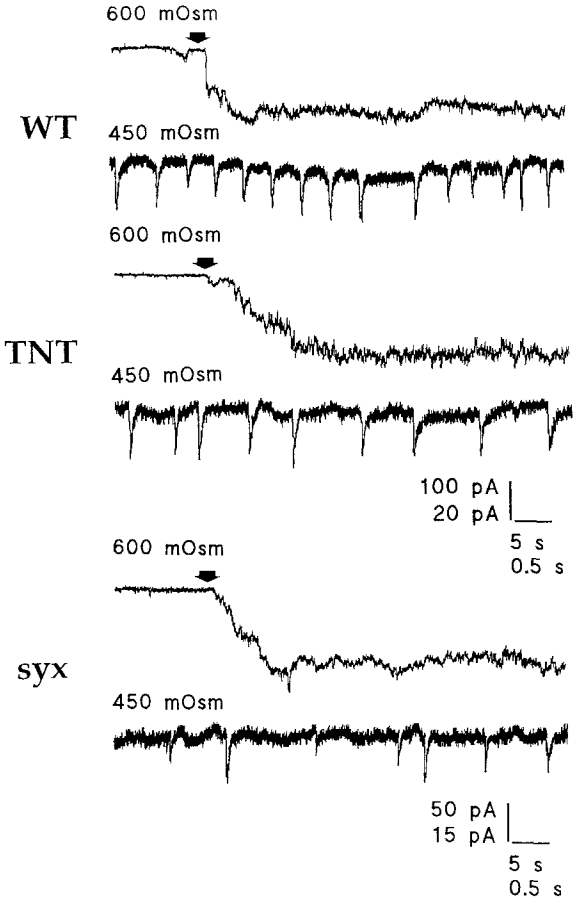

Figure 6. Hyperosmotic Saline Induces the Fusion of Synaptic Vesicles at the Embryonic NMJ in the Absence of Either n-Synaptobrevin or Syntaxin

A normal bath saline of 300 mOsm was used in all experiments. Two concentrations of hyperosmotic salines were pressure injected onto the muscles in the mature embryo (22–24 hr AEL): high osmolarity (600 mOsm; upper traces) and moderate osmolarity (450 mOsm; lower traces). In wild type (WT), application of 600 mOsm saline (arrow) induced mass exocytosis for the duration of application. Application of 450 mOsm saline (lower trace) induced high frequency MEJCs in which individual events can be clearly distinguished. In TNT, vesicle release in response to high osmolarity salines was indistinguishable from wild type. In syntaxin null mutants (*syx*), 450 mOsm saline induced clear MEJC events, though at a frequency reduced from normal. Similarly, application of 600 mOsm saline (arrow) induced mass exocytosis in *syx*, though the amplitude of this response was significantly reduced relative to wild type. In all three genotypes, very similar responses were observed with focal application of the Ca^{2+}–chelator EGTA in the range of 0.5–1.0 mM (data not shown).

osmotic saline stimulates high levels of vesicle release in a fashion similar to wild type (Figure 6). Likewise, in *syx*, application of hypertonic solutions can induce MEJCs although they are absent under normal conditions (compare Figures 5 and 6). At a 50% increase in osmolarity (from 300 to 450 mOsm), MEJCs occur in *syx* but remain very rare events relative to wild type and show a much greater variation in amplitude (Figure 6). Both classes of MEJCs are observed, and both classes show a similar time course to wild-type events. If more elevated osmolarity saline (600 mOsm) is applied, mass exocytosis can be triggered in *syx* similar to wild type (Figure 6), though the amplitude of this event is invariably smaller. Whether this amplitude difference is due to the decreased number of synaptic boutons in *syx* (Figure 1E) or a decreased likelihood of vesicle fusion remains unknown. However, these results support the finding of docked vesicles in *syx* and demonstrate these vesicles to be mature and functional.

Discussion

Syntaxin and n-Synaptobrevin Function Downstream of Vesicle Docking as Judged by Ultrastructural Analysis and Quantal Release

In Drosophila synapses, removal of syntaxin or n-synaptobrevin blocks transmission downstream of vesicle docking. First, we showed that *syx* and TNT do not interfere with NMJ development and architecture as judged by protein localizations and morphological appearance in the light microscope. This statement is qualified by the observation that the number of synaptic boutons is reduced in *syx* mutants. Second, in wild-type, *syx*, and TNT NMJs, ultrastructural analyses revealed synaptic vesicles in direct physical contact with the specialized presynaptic release sites, which are known to show exocytotic figures (Jia et al., 1993). In agreement with comparable descriptions for vertebrates and other invertebrates (e.g., Heuser et al., 1979; Bommert et al., 1993; Hess et al., 1993; Hunt et al., 1994; DeBello et al., 1995), we consider such vesicles as docked. Third, the significance of our ultrastructural findings is supported by the electrophysiological results showing that MEJCs persist in TNT, strongly suggesting the presence of a docked vesicle population competent to fuse. Finally, MEJCs can be stimulated by hyperosmotic saline in *syx*. Such MEJCs have been demonstrated to be due to fusion of the restricted pool of docked vesicles (Stevens and Tsujimoto, 1995). Thus, by both ultrastructural and electrophysiological criteria, vesicles dock at release sites in the absence of syntaxin and synaptobrevin.

Our electrophysiological conclusions rest on the classical assumption that MEJCs represent spontaneous vesicle fusion. However, at the Drosophila NMJ, the nature of MEJCs has been somewhat unclear (Broadie et al., 1994; Kidikoro and Nishikawa, 1994). A problem arises since stimulation of the late embryonic NMJ in low Ca^{2+} results in the release of single quantum that activates only a few (two to four) postsynaptic receptors (Broadie et al., 1994). This small response appears to be due to the sparse postsynaptic receptor field, limiting quantal response at the developing synapse, and has been similarly demonstrated at newly developing vertebrate NMJs (Evers et al., 1989). In contrast, in the presence of Ca^{2+}, much larger spontaneous MEJCs (activation of 15–20 receptors) have been described as representing quantal events (Kidikoro and Nishikawa, 1994). However, these large MEJCs do not appear to represent quanta for several reasons: they are strongly Ca^{2+} dependent, they are interspersed with a large number of smaller events, they can often be resolved into smaller quanta (summation), and they are much larger than the minimal quanta evoked by stimulation (Broadie

et al., 1994; Kidikoro and Nishikawa, 1994). Thus, these large MEJCs appear to be the sum of synchronously released quanta.

Owing to this complication, we have restricted our analyses to Ca^{2+}-free conditions. In the absence of Ca^{2+}, the large MEJCs are essentially absent but two populations of quantal MEJCs are still observed (Figure 4A): class 1, rare MEJCs with large amplitude and rapid time course: class 2, relatively frequent MEJCs with smaller amplitude and markedly slower time course. In the light of recent reports that ventral muscles in the Drosophila embryo are electrically coupled (Gho, 1994; Kidikoro and Nishikawa, 1994), these different populations of MEJCs can now be interpreted as quanta released onto the clamped muscle fiber (class 1) and as quanta released onto a number of coupled neighboring muscle fibers (class 2). According to this hypothesis, the higher frequency of class 2 MEJCs arises since they represent quanta released at a number of NMJs on coupled fibers, and the electrical characteristics of class 2 MEJCs arise from electrical filtering occurring at muscle fiber junctions (Figure 4A). Attempts to test this hypothesis, by uncoupling muscles following the methods of Gho (1994), have so far failed owing to an increase in background noise (K. B., unpublished data). Nevertheless, we suggest that the MEJCs reported here and in previous studies (Broadie et al., 1994; Sweeney et al., 1995) represent spontaneous vesicle release onto a group of coupled muscle fibers.

Syntaxin, Synaptobrevin, and the SNARE Hypothesis

Our observations suggest that the SNARE hypothesis does not adequately describe vesicle targeting or docking during synaptic transmission, at least in Drosophila. An alternative possibility is that other SNAREs exist in these synapses. For example, another member of the syntaxin protein family (Bennett et al., 1993) may be present that plays a t-SNARE docking role distinct from the role of the syntaxin protein described here. Alternatively, syntaxin may have a functionally redundant docking role with SNAP-25 that has been proposed as another presynaptic t-SNARE (Söllner et al., 1993a, 1993b) and is known to be present in Drosophila (Schulze et al., 1995). Since synaptobrevin normally forms a complex with both syntaxin and SNAP-25 (Hayashi et al., 1994), it is possible that either syntaxin or SNAP-25 alone is sufficient to mediate synaptic vesicle docking at active zones. The strongest candidate for a distinct v-SNARE is synaptotagmin, another integral vesicle protein that binds syntaxin (Bennett et al., 1992). However, in Drosophila, some evoked vesicle fusion persists in the absence of synaptotagmin (Broadie et al., 1994), suggesting that targeted vesicle docking must persist. A recent study of synaptotagmin I null mutants in mice also shows no defect in vesicle docking (Geppert et al., 1994). Thus, genetic deletion of each of these SNAREs (syntaxin, synaptobrevin, and synaptotagmin) has failed to reveal a vesicle docking function for these proteins, though each protein plays other essential roles in synaptic transmission. We conclude that the simple SNARE hypothesis is probably not sufficient to describe vesicle targeting in synaptic transmission without recourse to combinatorial models involving several proteins.

Synaptobrevin Functions Downstream of Docking but Upstream of Fusion

In Drosophila, n-synaptobrevin plays an essential role in synaptic transmission that is downstream of vesicle docking. In the absence of functional n-synaptobrevin, clustered vesicles accumulate near release sites and docked to the presynaptic membrane (Table 1), in agreement with earlier studies showing an arrest of docked vesicles upon TNT injection in the squid synapse (Hunt et al., 1994). In the absence of n-synaptobrevin, evoked fusion of synaptic vesicles cannot be elicited by either depolarization or other Ca^{2+}-dependent and Ca^{2+}-independent signals (i.e., latroinsectotoxin). These observations suggest that the protein acts downstream of the Ca^{2+} signaling pathway per se and downstream of the latrotoxin regulatory level. As shown for vertebrates, latrotoxin-induced release is triggered via interaction with neurexins (Petrenko, 1993; Petrenko et al., 1993). On the other hand, spontaneous vesicle fusion persists in the absence of n-synaptobrevin, suggesting that vesicles can undergo apparently normal fusion at release sites in the absence of the protein. Therefore, n-synaptobrevin is not required for synaptic vesicle fusion. We conclude that n-synaptobrevin is required to present the vesicle in an evoked fusion-competent state somewhere between receipt of the fusion signal (downstream of neurexin function) and the actual fusion step. The precise nature of this requirement remains unclear, but it is possible that synaptobrevin acts as a vesicle-associated regulator of evoked fusion through its interaction with the core proteins of the presynaptic fusion complex, such as syntaxin and SNAP-25 (Hayashi et al., 1994). One attractive possibility is that n-synaptobrevin acts to mediate the interaction of the syntaxin–SNAP-25 complex to the Ca^{2+}-sensing machinery (e.g., synaptotagmin) during evoked vesicle fusion.

Syntaxin Plays a Role in Fusion

In the absence of syntaxin, neither evoked nor spontaneous fusion occurs at the NMJ, although release sites look perfectly normal at the ultrastructural level and show docked vesicles. In addition, synaptic vesicle fusion cannot be stimulated by latroinsectotoxin, suggesting syntaxin functions downstream of neurexins. Instead, fusion can only be triggered by completely nonspecific stimuli, such as hyperosmotic saline. Since such stimuli are thought to release docked vesicles only (Stevens and Tsujimoto, 1995), the docked synaptic vesicles in *syx* appear to be mature and ready for fusion. However, in the absence of syntaxin, fusion fails to occur and docked synaptic vesicles accumulate at the presynaptic membrane (Table 1).

Taken together, these data strongly suggest that syntaxin is required for the actual fusion event between vesicle and plasma membranes. Syntaxin is not only part of the specialized machinery underlying synaptic transmission, but appears to play a more general role in the ancestral

exocytosis pathway, as it is required for both neuronal and nonneuronal exocytosis (Schulze et al., 1995). Therefore, we suggest that syntaxin forms the central core of the molecular machine that allows fusion between vesicle and plasma membranes in all exocytotically active cells. This hypothesis would explain why syntaxin binds directly to most of the other components of the fusion complex, providing a direct link between the plasma membrane, vesicle membrane, and regulators of the fusion event such as the Ca^{2+} channel, putative Ca^{2+} sensor (synaptotagmin), and associated factors (n-Sec1, synaptobrevin, SNAP-25, et cetera). This hypothesis would also explain the mutant phenotype in Drosophila, with its absence of both induced and noninduced vesicle fusion both at the synapse and in other tissues (Schulze et al., 1995). It would be predicted that such a central role of syntaxin in vesicle fusion might result in a cell-lethal phenotype, as indeed has been demonstrated for rop (Drosophila homolog of n-Sec1), a syntaxin-binding protein (Harrison et al., 1994). In the case of both *rop* and *syx* mutants, it is likely that survival into the late embryo is permitted owing only to the large contribution of maternal protein earlier in development (K. B., unpublished data).

In conclusion, genetic manipulations in Drosophila show that both syntaxin and n-synaptobrevin play essential roles in synaptic transmission. However, neither protein plays the synaptic vesicle docking role predicted by the SNARE hypothesis. Instead, both proteins play distinct, essential roles downstream of vesicle docking. Synaptobrevin plays a role specific to the synapse and is required somewhere between receipt of the evoked fusion signal and the actual fusion event. Syntaxin plays a role in the general ancestral exocytosis pathway and is likely to be required for the actual fusion event between vesicle and plasma membranes in all cells.

Experimental Procedures

Drosophila Genotypes

We used three genotypes in this study: wild-type (Oregon-R), *syx-1A* mutants, and trangenic lines expressing TNT throughout the nervous system. We used a strong hypomorphic allele of *syx-1A* (P[*syx*]), and a null mutation (syx^{229}) that completely eliminates mRNA and protein expression (Schulze et al., 1995). Tetanus neurotoxin (TNT), which cleaves synaptobrevin (Niemann et al., 1994), was expressed in the nervous system of transgenic Drosophila embryos (Sweeney et al., 1995). Flies homozygous for a yeast *gal4* gene insert, 1407 (courtesy of J. Urban; see Brand and Perrimon, 1993) were crossed to flies homozygous for a construct of TNT light chain (catalytic domain; Niemann et al., 1994) coupled to the yeast UAS promoter. All offspring of this cross (TNT embryos) express catalytically active TNT light chain throughout the nervous system, which eliminates all detectable n-synaptobrevin protein at the NMJ (Sweeney et al., 1995).

For all genotypes, analyses were done on mature embryos at the end of embryogenesis (22–24 hr after egg laying [AEL]). Eggs were collected at hourly intervals, then dechorionated in commercial bleach, staged as gastrulae (3 hr AEL), and incubated in a humid chamber at 25°C to the desired age. Mutant genotypes were determined by a combination of morphological phenotype, the use of marked balancer chromosomes, or immunocytochemical staining for TNT, n-synaptobrevin, or syntaxin as described previously (Schulze et al., 1995; Sweeney et al., 1995).

Histology

Staged embryos and larvae were immunocytochemically stained as reported previously (Broadie and Bate, 1993a). In brief, animals were dissected along the dorsal midline, internal organs removed, and the preparation fixed flat for 30 min with 4% paraformaldehyde. The preparations were probed with a polyclonal anti–fasciclin II antibody (1:10), which recognizes the cytoplasmic domain of fasciclin II in all motor neurons (Van Vactor et al., 1993); with a monoclonal anti-TNT antibody (1:5000), which recognizes the transgenic toxin (Sweeney et al., 1995); with a polyclonal anti-synaptotagmin antibody (1:1000; Littleton et al., 1993); with a polyclonal anti-rat syn-1A protein (1:100), which recognized the Drosophila syn-1A protein (Schulze et al., 1995); with a monoclonal anti–cysteine string protein antibody (1:10; Zinsmaier et al., 1990); or with a polyclonal antibody against the HV62 peptide containing residues 33–94 of human synaptobrevin 2 (1:500; Shone et al., 1993), which recognizes the Drosophila n-synaptobrevin protein (Sweeney et al., 1995). The staining was visualized using a Vectastain ABC Elite kit as reported previously (Broadie and Bate, 1993a, 1993b).

Electrophysiology

Electrophysiology was pursued at an identified NMJ on muscle 6 in the anterior abdomen (A2–A3) of mature embryos (22–24 hr AEL) as reported previously (Broadie and Bate, 1993a, 1993b). Whole-cell recordings of muscle 6 were made using standard patch–clamp techniques. The muscle was voltage clamped at −60 mV. Signals were amplified using an Axpatch-1D (Axon Instruments) patch–clamp amplifier and filtered at 2 kHz. Data was analyzed using pCLAMP 5.51 software (Axon Instruments). The genotype of embryos was confirmed following recording with the use of marked balancer chromosomes or immunocytochemical staining for TNT, n-synaptobrevin, or syntaxin.

The postsynaptic current was studied by L-glutamate iontophoresis as reported previously (Broadie and Bate, 1993a, 1993b). In brief, a solution of 0.1 M L-glutamate was focally applied to the NMJ with short pulses (10 ms) of negative current and the resulting current measured in the voltage-clamped muscle. The EJC was studied by stimulating the motor nerve with a suction electrode near where it exits the CNS and recording the synaptic current in the voltage-clamped muscle, as reported previously (Broadie and Bate, 1993a). Spontaneous MEJCs were studied after the motor nerve was cut, and recordings were made in 0 mM Ca^{2+} saline buffered with 0.1 mM EGTA, as reported previously (Broadie et al., 1994; Sweeney et al., 1995).

The latroinsectotoxin response was measured as follows: frozen BWSV glands were obtained from Sigma, homogenized in a ground glass homogenizer, and filtered through a Millipore filter (0.2 μm). The toxin was applied directly to the muscles with a pressure pipette during continuous monitoring of MEJC frequency. The venom was applied either in the presence of external Ca^{2+} (1.0 mM) or Ca^{2+}-free bath (buffered with 0.1 mM EGTA).

The response to hyperosmotic salines was measured as follows: dissected embryos were maintained in a bath saline at 300 mOsm, within the range of normal Drosophila salines (Stewart et al., 1994). High osmolarity salines (range of 350–600 mOsm) were applied directly to the muscles with a pressure pipette during continuous recording of MEJC frequency. The osmolarity of the applied saline was regulated with sucrose (Sigma; 99.9% pure). Saline containing EGTA (range 0.5–2.0 mM) was applied in a similar fashion.

Electron Microscopy

Specimens for all three genotypes were generated in two ways: either dissected embryo flat preparations (Broadie and Bate, 1993a) were fixed in Trump's fixative, then postfixed, dehydrated, and embedded following a standard protocol for larval NMJs (Atwood et al., 1993; Jia et al., 1993), or intact embryos were injected (for details see Prokop and Technau, 1993) with 5% glutaraldehyde in 0.05M phosphate buffer (PB), followed by 1 hr postfixation in 2.5% glutaraldehyde in 0.05 M PB. Owing to the thin cuticula (Schulze et al., 1995), *syx* embryos were not injected but were mechanically devitellinized and directly incubated in the postfix solution. Preparations were briefly washed in 0.05 M PB, fixed for 1 hr in 1% osmium in dH_2O, washed in dH_2O for 10 min, treated en bloc with an aqueous 2% solution of uranyl acetate, dehydrated, and embedded in araldite. Serial sections (30–50 nm; gray to silver) were transferred to carbonated Formvar-coated slot grids following the method of Galey and Nilsson (1966), postcontrasted with lead citrate for 5–10 min, and analyzed on a Phillips EM300 or Jeol 200CX.

For electron microscopic statistics, vesicles at ultrastructurally defined NMJ release sites were counted. Clustered vesicles were counted that were within 180 nm (5-vesicle diameters) of the electron-dense presynaptic membrane. Docked vesicles were counted as those vesicles within 40 nm (<1-vesicle diameter) range from the presynaptic membrane. Significance was analyzed using Mann–Whitney U tests.

Acknowledgments

K. B. and A. P. contributed equally to this work. All other authors contributed similarly to this work and are listed alphabetically. We are especially grateful to M. Bate, in whose laboratory this work was done. A. P. would like to thank M. Day, H. Skaer, J. Skepper, and especially B. Leitch for helpful advice on electron microscopic techniques. K. B. is a research fellow at Girton College, Cambridge, England, whose work is supported by The Wellcome Trust. A. P. is supported by a Human Capital and Mobility grant. H. J. B. is an Assistant Investigator of the Howard Hughes Medical Institute. S. T. S. is supported by a studentship from the Biotechnology and Biological Sciences Research Council.

The costs of publication of this article were defrayed in part by the payment of page charges. This article must therefore be hereby marked "*advertisement*" in accordance with 18 USC Section 1734 solely to indicate this fact.

Received March 22, 1995; revised June 14, 1995.

References

Atwood, H. L., Govind, C. K., and Wu, C.-F. (1993). Neuromuscular junction ultrastructure of ventral abdominal muscles in *Drosophila* larvae. J. Neurobiol. *24*, 1008–1024.

Bekkers, J. M., and Stevens, C. F. (1989). NMDA and non-NMDA receptors are co-localized at individual excitatory synapses in cultured rat hippocampus. Nature *341*, 230–233.

Bennett, M. K., and Scheller, R. H. (1994). A molecular description of synaptic vesicle membrane trafficking. Annu. Rev. Biochem. *63*, 63–100.

Bennett, M. K., Calakos, N., and Scheller, R. H. (1992). Syntaxin: a synaptic vesicle protein implicated in the docking of synaptic vesicles at presynaptic active zones. Science *257*, 255–259.

Bennett, M. K., Garcia-Arraras, J. E., Elferink, L. A., Peterson, K., Fleming, A. M., Hazuka, C. D., and Scheller, R. H. (1993). The syntaxin family of vesicular transport receptors. Cell *74*, 863–873.

Blasi, J., Chapman, E. R., Yamaski, S., Binz, T., Niemann, H., and Jahn, R. (1993). Botulinum neurotoxin C1 blocks neurotransmitter release by means of cleaving HPC-1/syntaxin. EMBO J. *12*, 4821–4828.

Bommert, K., Charlton, M. P., DeBello, W. M., Chin, G. J., Betz, H., and Augustine, G. J. (1993). Inhibition of neurotransmitter release by C2-domain peptides implicates synpatotagmin in exocytosis. Nature *363*, 163–165.

Brand, A. H., and Perrimon, N. (1993). Targeted gene expression as a means of altering cell fates and generating dominant phenotypes. Development *118*, 401–415.

Broadie, K. (1994). Synaptogenesis in *Drosophila*: coupling genetics and electrophysiology. J. Physiol. *88*, 123–139.

Broadie, K. (1995). Genetic dissection of the molecular mechanisms of transmitter vesicle release during synaptic transmission. J. Physiol. *89*, 59–70.

Broadie K., and Bate, M. (1993a). Development of the embryonic neuromuscular synapse of *Drosophila melanogaster*. J. Neurosci. *13*, 144–166.

Broadie, K., and Bate, M. (1993b). Activity-dependent development of the neuromuscular synapse during Drosophila embryogenesis. Neuron *11*, 607–619.

Broadie K., Bellen, H. J., DiAntonio, A., Littleton, J. T., and Schwarz, T. L. (1994). The absence of synaptotagmin disrupts excitation-secretion coupling during synaptic transmission. Proc. Natl. Acad. Sci. USA *91*, 10727–10731.

Chen, A. C., Burgess, R. W., Wang, B. R., Schwarz, T. L., and Scheller, R. H. (1993). Differential expression of transcripts from *syb*, a *Drosophila melanogaster* gene encoding VAMP (synaptobrevin) that is abundant in non-neuronal cells. Gene *131*, 175–181.

Clark, A. W., Mauro, A., Longenecker, H. E., and Hurlbut, W. P. (1970). Effects of black widow spider venom on the frog neuromuscular junction: effects on the fine structure. Nature *225*, 703.

Clark, A. W., Hurlbut, W. P., and Mauro, A. (1972). Changes in the fine structure of the neuromuscular junction of the frog caused by black widow spider venom. J. Cell Biol. *52*, 1–14.

DeBello, W. M., O'Connor, V., Dresbach, T., Whiteheart, S. W., Wang, S. S.-H., Schweizer, F. E., Betz, H., Rothman, J. E., and Augustine, G. J. (1995). SNAP-mediated protein–protein interactions essential for neurotransmitter release. Nature *373*, 626–630.

DiAntonio, A., Burgess, R., Chin, A. C., Deitcher, D. L., Scheller, R. H., and Schwarz, T. L. (1993). Identification and characterization of *Drosophila* genes for synaptic vesicle proteins. J. Neurosci. *13*, 4924–4935.

Evers, J., Laser, M., Sun, Y., Xie, Z., and Poo, M.-m. (1989). Studies of nerve–muscle interactions in *Xenopus* cell culture: analysis of early synaptic currents. J. Neurosci. *9*, 1523–1539.

Furshpan, E. J. (1956). The effects of osmotic pressure on the spontaneous activity at motor nerve endings. J. Physiol. *134*, 689–697.

Galey, F. R., and Nilsson, S. E. G. (1966). A new method for transferring sections from the liquid surface of the trough through staining solutions to the supporting film of a grid. J. Ultrastruct. Res. *14*, 405–410.

Geppert, M., Goda, Y., Hammer, R. E., Li, C., Rosahl, T. W., Stevens, C. F., and Südhof, T. C. (1994). Synaptotagmin I: a major Ca^{2+} sensor for transmitter release at a central synapse. Cell *79*, 717–727.

Gho, M. (1994). Voltage-clamp analysis of gap-junctions between embryonic muscles in *Drosophila*. J. Physiol. *481*, 371–383.

Govind, C. K., DeRosa, R. A., and Pearce, J. (1980). Presynaptic dense bars at neuromuscular synapses of the lobster, *Homarus americanus*. Cell Tissue Res. *207*, 81–88.

Harrison, S. D., Broadie, K., van de Goor, J., and Rubin, G. M. (1994). Mutations in the Drosophila *Rop* gene suggest a function in general secretion and synaptic transmission. Neuron *13*, 555–566.

Hayashi, T., McMahon, H., Yamasaki, S., Binz, T., Hata, Y., and Südhof, T. C. (1994). Synaptic vesicle membrane-fusion complex: action of clostidial neurotoxins on assembly. EMBO J. *13*, 5051–5061.

Hess, S. D., Doroshenko, P. A., and Augustine, G. J. (1993). A functional role for GTP-binding proteins in synaptic vesicle cycling. Science *259*, 1169–1172.

Heuser, J. E., and Reese, T. S. (1973). Evidence for recycling of synaptic vesicle membrane during transmitter release at the frog neuromuscular junction. J. Cell Biol. *57*, 315–344.

Heuser, J. E., Reese, T. S., Dennis, M. J., Jan, Y., Jan, L., and Evans, L. (1979). Synaptic vesicle exocytosis captured by quick freezing and correlated with quantal transmitter release. J. Cell Biol. *81*, 275–300.

Hunt, J. M., Bommert, K., Charlton, M. P., Kistner, A., Habermann, E., Augustine, G. J., and Betz, H. (1994). A postdocking role for synaptobrevin in synaptic vesicle fusion. Neuron *12*, 1269–1279.

Jahn, R., and Südhof, T. C. (1994). Synaptic vesicles and exocytosis. Annu. Rev. Neurosci. *17*, 219–246.

Jia, X.-X., Gorczyca, M., and Budnik, V. J. (1993). Ultrastructure of neuromuscular-junctions in *Drosophila*: comparison of wild-type and mutants with increased excitability. J. Neurobiol. *24*, 1025–1044.

Johansen, J., Halpern, M. E., Johansen, K., and Keshishian, H. (1989). Stereotypic morphology of glutamatergic synapses on identified muscle cells of *Drosophila* larvae. J. Neurosci. *9*, 710–725.

Kelly, R. B. (1993). Storage and release of neurotransmitters. Cell *72*/ Neuron *10* (Suppl.), 43–53.

Kidikoro, Y., and Nishikawa, K. (1994). Miniature endplate currents at the newly formed neuromuscular junction in *Drosophila* embryos and larvae. Neurosci. Res. *19*, 143–154.

Lahey, T., Gorczyca, M., Jia, X.-X., and Budnik, V. (1994). The Dro-

sophila tumor suppressor gene *dlg* is required for normal synaptic bouton structure. Neuron *13*, 823–835.

Littleton, J. T., Bellen, H. J., and Perin, M. S. (1993). Expression of synaptotagmin in *Drosophila* reveals transport and localization of synaptic vesicles in the synapse. Development *118*, 1077–1088.

Magazanik, L. G., Fedorova, I. M., Kovalevskaya, G. I., Pashkov, V. N., Bulgakov, O. V., and Grishin, E. V. (1992). Selective presynaptic insectotoxin (α-latroinsectotoxin) isolated from black widow spider venom. Neuroscience *46*, 181–188.

Niemann, H., Blasi, J., and Jahn, R. (1994). Clostridial neurotoxins: new tools for dissecting exocytosis. Trends Cell Biol. *4*, 179–185.

Niles, W. D., and Smith, D. O. (1982). Effects of hyperosmotic solutions on quantal transmitter release at the crayfish neuromuscular junction. J. Physiol. *329*, 185–202.

Osborne, M. P. (1967). The fine structure of neuromuscular junctions in the segmental muscles of the blowfly larva. J. Insect Physiol. *13*, 827–833.

Osborne, M. P. (1975). The ultrastructure of nerve muscle synapses. In Insect Muscle, P. N. R. Usherwood, ed. (New York: Academic Press), pp. 151–205.

Petrenko, A. G. (1993). α-Latrotoxin receptor: implications in nerve terminal function. FEBS Lett. *325*, 81–85.

Petrenko, A. G., Lazaryeava, V. D., Geppert, M., Tarasyuk, T. A., Moomaw, C., Ushkaryov, Y. A., Slaughter, C., Nasimov, I. V., and Südhof, T.C. (1993). Polypeptide composition of the α-latrotoxin receptor: a high affinity binding-protein consists of a family of related high molecular weight polypeptides. J. Biol. Chem. *268*, 1860–1867.

Pevsner, J., Hsu, S.-C., and Scheller, R. H. (1994). n-Sec1: a neural-specific syntaxin-binding protein. Proc. Natl. Acad. Sci. USA *91*, 1445–1449.

Probst, J. W., and Ko, C.-P. (1987). Correlations between active zone ultrastructure and synaptic function studied with freeze-fracture of physiologically identified neuromuscular junctions. J. Neurosci. *7*, 3654–3664.

Prokop, A., and Technau, G. H. (1993). Cell transplantations. In Cellular Interactions in Development: A Practical Approach, D. Hartley, ed. (London: Oxford University Press), pp. 33–57.

Ramaswami, M., Krishnan, K. S., and Kelly, R. B. (1994). Intermediates in synaptic vesicle recycling revealed by optical imaging of Drosophila neuromuscular junction. Neuron *13*, 363–375.

Schulze, K. L., Broadie, K., Perin, M. S., and Bellen, H. J. (1995). Genetic and electrophysiological studies of Drosophila syntaxin-1A demonstrate its role in nonneuronal secretion and its essential role in neurotransmitter release. Cell *80*, 311–320.

Shone, C. C., Quinn, C. P., Wait, R., Hallis, B., Fooks, S. G., and Hambleton, P. (1993). Proteolytic cleavage of synthetic fragments of vesicle-associated membrane protein isoform-2 by botulinum type B neurotoxin. Eur. J. Biochem. *217*, 965–971.

Söllner, T., Bennett, M. K., Whitehart, S. W., Scheller, R. H., and Rothman, J. E. (1993a). A protein assembly–disassembly pathway in vitro that may correspond to sequential steps of synaptic vesicle docking, activation and fusion. Cell *75*, 409–418.

Söllner, T., Whiteheart, S. W., Brunner, M., Erdjument-Bromage, H., Geromanos, S., Tempst, P., and Rothman, J. E. (1993b). SNAP receptors implicated in vesicle targeting and fusion. Nature *362*, 318–324.

Stevens, C. F., and Tsujimoto, T. (1995). Estimates for the pool size of releasable quanta at a single central synapse and for the time required to refill the pool. Proc. Natl. Acad. Sci. USA *92*, 846–849.

Stewart, B. A., Atwood, H. L., Renger, J. J., Wang, J., and Wu, C.-F. (1994). Improved stability of *Drosophila* neuromuscular preparations in haemolymph-like physiological salines. J. Comp. Physiol. (A) *175*, 179–191.

Sweeney, S. T., Broadie, K., Keane, J., Niemann, H., and O'Kane, C. J. (1995). Targeted expression of tetanus toxin light chain in Drosophila specifically eliminates synaptic transmission and causes behavioral defects. Neuron *14*, 341–351.

Van Vactor, D., Sink, H., Fambrough, D., Tsoo, R., and Goodman, C. S. (1993). Genes that control neuromuscular specificity in Drosophila. Cell *73*, 1137–1153.

Zinsmaier, K., Hofbauer, A., Heimbeck, G., Pflugfelder, G., Buchner, S., and Buchner, E. (1990). A cysteine-string protein is expressed in retina and brain of *Drosophila*. J. Neurogenet. *7*, 15–29.